



The faecal microbiome of the Australian silver gull contains phylogenetically diverse ExPEC, aEPEC and *Escherichia coli* carrying the transmissible locus of stress tolerance

Ethan R. Wyrsh^a, Bethany J. Hoye^b, Martina Sanderson-Smith^c, Jody Gorman^c, Kimberly Maute^b, Max L. Cummins^a, Veronica M. Jarocki^a, Marc S. Marendá^d, Monika Dolejska^{e,f,g,h}, Steven P. Djordjevic^{a,*}

^a Australian Institute for Microbiology and Infection, University of Technology Sydney, Ultimo, NSW, Australia

^b School of Earth, Atmospheric and Life Sciences, Faculty of Science, Medicine and Health, University of Wollongong, Wollongong, NSW, Australia

^c Molecular Horizons Research Institute, School of Chemistry and Molecular Bioscience, University of Wollongong, Wollongong, NSW, Australia

^d Department of Veterinary Biosciences, Faculty of Veterinary and Agricultural Sciences, The University of Melbourne, Werribee, VIC 3030, Australia

^e Department of Biology and Wildlife Diseases, Faculty of Veterinary Hygiene and Ecology, University of Veterinary Sciences Brno, Czech Republic

^f CEITEC VETUNI, University of Veterinary Sciences Brno, Czech Republic

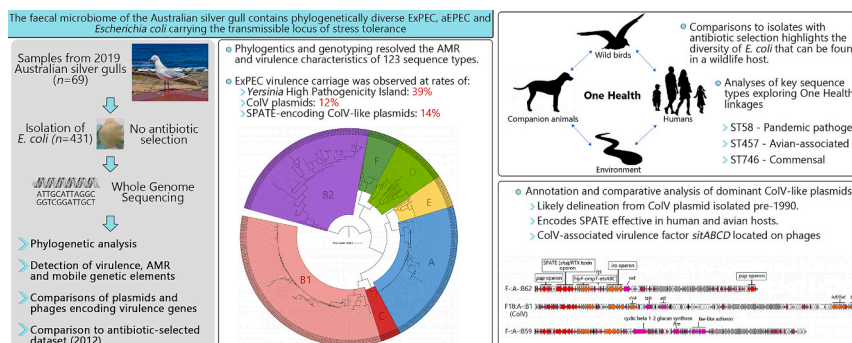
^g Department of Clinical Microbiology and Immunology, Institute of Laboratory Medicine, The University Hospital Brno, Czech Republic

^h Department of Microbiology, Faculty of Medicine and University Hospital in Plzen, Charles University, Pilsen, Czech Republic

HIGHLIGHTS

- *Escherichia coli* from major phylogroups identified, with prominent B2 carriage
- Expansive collection of 123 sequence types with multiple pathogens identified
- Frequent isolation of extraintestinal pathogenic *Escherichia coli*
- Diverse *E. coli* carry the transmissible locus of stress tolerance.
- Epidemiological linkages between humans and animals across multiple lineages

GRAPHICAL ABSTRACT



ARTICLE INFO

Editor: Ewa Korzeniewska

Keywords:
Bacteria
Escherichia coli
Virulence
Epidemiology

ABSTRACT

Wildlife are implicated in the dissemination of antimicrobial resistance, but their roles as hosts for *Escherichia coli* that pose a threat to human and animal health is limited. Gulls (family Laridae) in particular, are known to carry diverse lineages of multiple-antibiotic resistant *E. coli*, including extra-intestinal pathogenic *E. coli* (ExPEC). Whole genome sequencing of 431 *E. coli* isolates from 69 healthy Australian silver gulls (*Chroicocephalus novaehollandiae*) sampled during the 2019 breeding season, and without antibiotic selection, was undertaken to assess carriage in an urban wildlife population. Phylogenetic analysis and genotyping resolved 123 sequence

Abbreviations: ExPEC, extraintestinal pathogenic *Escherichia coli*; aEPEC, atypical enteropathogenic *Escherichia coli*.

* Corresponding author.

E-mail address: Steven.Djordjevic@uts.edu.au (S.P. Djordjevic).

<https://doi.org/10.1016/j.scitotenv.2024.170815>

Received 5 December 2023; Received in revised form 28 January 2024; Accepted 6 February 2024

Available online 7 February 2024

0048-9697/© 2024 The Authors. Published by Elsevier B.V. This is an open access article under the CC BY license (<http://creativecommons.org/licenses/by/4.0/>).

Genome sequencing
AMR

types (STs) representing most phylogroups, and identified diverse ExPEC, including an expansive phylogroup B2 cluster comprising 103 isolates (24 %; 31 STs). Analysis of the mobilome identified: i) widespread carriage of the *Yersinia* High Pathogenicity Island (HPI), a key ExPEC virulence determinant; ii) broad distribution of two novel phage elements, each carrying *sitABCD* and iii) carriage of the transmissible locus of stress tolerance (tLST), an element linked to sanitation resistance. Of the 169 HPI carrying isolates, 49 (48 %) represented diverse B2 isolates hosting FII-64 ColV-like plasmids that lacked *iutABC* and *sitABC* operons typical of ColV plasmids, but carried the serine protease autotransporter gene, *sha*. Diverse *E. coli* also carried archetypal ColV plasmids (52 isolates; 12 %). Clusters of closely related *E. coli* (<50 SNVs) from ST58, ST457 and ST746, sourced from healthy gulls, humans, and companion animals, were frequently identified. In summary, anthropogenically impacted gulls host an expansive *E. coli* population, including: i) putative ExPEC that carry ColV virulence gene cargo (101 isolates; 23.4 %) and HPI (169 isolates; 39 %); ii) atypical enteropathogenic *E. coli* (EPEC) (17 isolates; 3.9 %), and iii) *E. coli* that carry the tLST (20 isolates; 4.6 %). Gulls play an important role in the evolution and transmission of *E. coli* that impact human health.

1. Introduction

Wildlife, particularly synanthropic species that persist and thrive in urban environments, carry a wide range of zoonotic pathogens (Albery et al., 2022; Hassell et al., 2017), and harbour increased levels of antimicrobial resistance (AMR) (Hassell et al., 2019; Furness et al., 2017; Uea-Anuwong et al., 2023; Tarabai, 2023; Dias et al., 2022; Nesporova et al., 2020). In these environments, exposure to human-contaminants, particularly municipal waste and wastewater, has been associated with increased risk of exposure to resistant organisms (Ahlstrom et al., 2021; Ahlstrom et al., 2019). Synanthropic wildlife are therefore recognised as a potentially important component of the epidemiology of antimicrobial resistance (Torres et al., 2021; Ramey and Ahlstrom, 2020; Dolejska and Literak, 2019; Cummins et al., 2020). However, a functional understanding of AMR transmission pathways and the magnitude of their influence from a One Health perspective remains unclear (Ramey and Ahlstrom, 2020). Similarly, the role of wildlife in the carriage of virulence and other stress-response genes remains under-explored (Lagerstrom and Hadly, 2021; Bolzoni and De Leo, 2013; Becker and Hall, 2014; Djordjevic, 2023).

Recent bacterial whole genome sequencing (WGS) studies from synanthropic wildlife, such as those exploring *Escherichia coli* isolated from the Australian Silver Gull (*Chroicocephalus novaehollandiae*), have demonstrated diverse lineages that harbour genes encoding resistance to clinically important antibiotics (Nesporova et al., 2020; Tarabai, 2023; Mukerji et al., 2020; Medvecky et al., 2022; Wyrsh et al., 2022a). For instance, *E. coli* isolated from the major breeding colony on Big Island (of the Five Islands Nature Reserve off the Illawarra coast of New South Wales), demonstrated broad and clinically important ARG profiles including carbapenem resistance gene *bla*_{IMP-4}, housed within a clinically widespread class 1 integron encoding the *bla*_{IMP-4}-*qacG*-*aacA4*-*catB3* array (Partridge et al., 2012), as well as a range of lineages (e.g. ST58, ST457 and ST131) with the capacity to cause extraintestinal disease in humans (Nesporova et al., 2020; Medvecky et al., 2022; Wyrsh et al., 2022a; Dolejska et al., 2016; Tarabai et al., 2021; Mukerji et al., 2019). Epidemic HI2 plasmids mobilising the carbapenemase gene *bla*_{IMP-4} in sublineages of ST216 have also been identified (Tarabai et al., 2021). However, Silver gulls sampled at remote sites, away from human populations, have been reported to be less likely to carry antibiotic resistance genes (ARGs) and to carry fewer genes per isolate (Mukerji et al., 2023), suggesting that carriage of ARGs in *E. coli* sampled from gulls is linked with anthropogenic activities.

Extraintestinal pathogenic *E. coli* (ExPEC) are the most frequently isolated Gram-negative pathogens globally (Poolman and Wacker, 2016) and the leading cause of urinary tract infections (UTIs) and blood stream infections in humans (Svanborg and Godaly, 1997) and companion animals (Elankumaran et al., 2022a). ExPEC are colonising opportunistic pathogens and as such are challenging to both define from a diagnostic standpoint, and to track from an epidemiological perspective. Nonetheless, ExPEC can be broadly defined by the combinations of virulence associated genes (VAGs) they carry. These VAGs are acquired

by lateral gene transfer, either as chromosomal islands (Johnson et al., 2018; Tu et al., 2016), phages (Venturini et al., 2019), or on plasmids (Cummins et al., 2022). The VAGs most often observed in cases of extraintestinal disease (humans and animals) are encoded by the *Yersinia* High Pathogenicity Island (HPI), a chromosomal island hosting the siderophores *irp* and *fyuA* (Galardini et al., 2020; Royer et al., 2023). Two groups of F family plasmids are also frequently associated with ExPEC. These include ColV and related plasmids (Cummins et al., 2022; Royer et al., 2023; Johnson and Nolan, 2009; T.J. Johnson et al., 2006; Reid et al., 2022) expressing microcin V, and plasmids that carry *cjrABC-senB* (typically pUTI89-like and related plasmids) that express the Colicin (Wyrsh et al., 2022a; Cummins et al., 2022; Reid et al., 2022; Cusumano et al., 2010; Wyrsh et al., 2022b). The identification of F plasmid RST types in combination with the presence of these VAGs has assisted greatly in the identification of potential ExPEC within larger datasets (Nesporova et al., 2020; Medvecky et al., 2022; Cummins et al., 2022; Royer et al., 2023; Reid et al., 2022).

ColV plasmids (named for the frequent presence of the microcin V operon) encompass a range of FII RST subtypes (Carattoli et al., 2014), including F2, F18, F24 and others, and variably encode a set of VAGs contributing to ExPEC pathogenesis. This includes the *iro* (salmochelin), *iut/iuc* (aerobactin) and *sit* operons for iron acquisition and transport, putative ABC transporter *ets*, immune evasion gene *iss*, plus outer membrane vesicle and protease production through *ompT* and *hlyF* (Reid et al., 2022). Numerous animal studies using murine and avian models of infection have underscored the importance of the virulence gene cargo on these plasmids in disease etiology (Royer et al., 2023; Skyberg et al., 2006; Liu et al., 2018; Murase et al., 2016). F virulence plasmids that are partially genetically related to ColV plasmids but that do not meet the strict definition afforded these plasmids have also been described. These F plasmids encode some of the VAGs that are typical of ColV plasmids but lack others, and often carry additional virulence content, including serine protease autotransporter protein (SPATEs) *Sha* (Pokharel et al., 2020). *Sha*, a Class 2 SPATE, possesses autoaggregation, hemagglutination and mucinase activity. In addition, internalisation of *Sha* by bladder epithelial cells causes actin rearrangement, and induces cytopathic effects (cell rounding), resulting in 6-fold upregulation of *Sha* expression in the bladder during UTI infection in mouse models (Habouria et al., 2019). *Sha* can increase biofilm formation at temperatures between 25 and 30 °C. These observations suggest the *E. coli* that harbour plasmids that carry these SPATEs require close monitoring as emerging ExPEC pathogens.

The other plasmid family, originally defined by pUTI89 (Cusumano et al., 2010), are most commonly observed as replicon subtype F29:A-B10 and encode tandem VAGs *cjrABC-senB*, but rarely ARGs (Cummins et al., 2022; Stephens et al., 2017). Variants of F29:A-B10 with distinct plasmid “backbones” and carriage of clinically important ARGs can be found in ST95 lineages (Cummins et al., 2022), ST131 clades A/H41 (Li et al., 2021), and in some lineages in B/H22 and clade C/H30 (Johnson et al., 2016). Modified F plasmids carrying *cjrABC-senB* that have lost part of their transposition module are dominant in ST1193, a recently

emerged pandemic ExPEC lineage (Wyrsh et al., 2022b; J.R. Johnson et al., 2019; T.J. Johnson et al., 2019). Other combinations of chromosomally hosted VAGs that are not well understood, may also contribute to ExPEC pathogenicity.

Here, we investigated the diversity, resistance and virulence of wildlife-sourced *E. coli*. Whole genome sequences were derived from a total of 431 *E. coli* isolates sourced from cloacal swabs of 69 Australian silver gulls sampled throughout their breeding season in 2019, representing the largest known collection of commensal *E. coli* from healthy gulls. Using these data, comparisons were made with a historical collection (2012) of whole genome sequences of 425 *E. coli* isolates from cloacal swabs of chicks inhabiting three coastal sites in New South Wales, including Big island, cultured on media supplemented with meropenem, cefotaxime, or ciprofloxacin.

2. Methods

2.1. Sample collection

Silver gulls were sampled on Big Island, Five Islands Nature Reserve, in the Illawarra region of NSW during the breeding season of 2019. Adults were captured on their nest using clap-traps during the incubation period. Once hatched, chicks were captured by hand from marked nests every 7–10 days after hatching. Birds were weighed, measured, and a cloacal swab collected using a rayon-tipped swab subsequently stored in amies (Copan, Italy). The handling of birds and collection of samples for bacterial analysis was conducted under approval from the University of Wollongong Animal Ethics Committee (AE17/20), the NSW National Parks and Wildlife Service (Scientific Licence 100,109), and the Australian Bird and Bat Banding Scheme (project 2731–03). Swabs were stored on ice while in the field (24–72 h) prior to culture.

2.2. Sample selection

Of the 505 cloacal swabs collected between 24th September and 24th November 2019, 226 were selected for inclusion in the study, including 34 swabs from adults (one sample event per adult) and 192 swabs from 59 chicks (1–6 sample events per chick).

2.3. Bacterial isolation and short-read whole genome sequencing

Swabs were placed in 1 ml LB broth, vortexed for 30s, then 10 μ l was streaked onto MacConkey agar (Edwards, Australia) and incubated overnight at 37 °C. All growth from each initial MacConkey agar plate was collected and stored at -80 °C in 1 ml of storage medium (milliQ water containing 1 % casamino acids and 10 % glycerol and autoclaved). These stored bacterial communities were diluted 10⁻⁹ in sterile PBS and 150 μ l was used to grow bacterial lawns on MacConkey agar. Five discrete lactose-fermenting colonies from these lawns were re-cultured overnight at 37 °C on Brilliant Green agar (Edwards, Australia). Cultures indicative of lactose/sucrose fermentation were re-cultured overnight at 37 °C in LB from which genomic DNA was extracted using the ISOLATE II Genomic DNA Kit (Bioline, Eveleigh, Australia) following the manufacturers standard protocol for bacterial cells and stored at -20 °C. An additional 15 colonies (i.e. 20 colonies in total) were collected from 7 swab samples – 3 from adult gulls and 4 from chicks. DNA library preparations were generated for short-read whole genome sequencing following the Hackflex protocol (Gaio et al., 2022), a modified version of the Illumina DNA preparation. Sequencing was performed on an Illumina NovaSeq 6000 platform. Short-read whole genome sequences were assembled using shovill v1.0.9 (<https://github.com/tseemann/shovill>).

2.4. Long-read whole genome sequencing

DNA extraction for long-read sequencing was performed from fresh

sub-cultures using a TANBead Maelstrom 4810 instrument and Tissue Lysis kit (ref. M6T2S46) after 1 h proteinase K digestion at 56C, according to the manufacturer's instructions. The sequencing library was prepared with the Oxford Nanopore kit SQK-RBK004, and was loaded on a R9.4.1 flowcell fitted on a MinION device running MinKNOW version 22.12.7. The basecalling was performed with Guppy version 6.4.6 using the High Accuracy model r9.4.1_450bps_hac. Demultiplexing and barcode trimming of the passed fastq files was performed with Guppy barcoding version 6.4.6. Reads were filtered for minimal length of 1 kb with Filtlong (<https://github.com/rrwick/Filtlong>). Eight hybrid short/long-read assemblies were generated using Unicycler v0.5.0 (Wick et al., 2017) (<https://github.com/rrwick/Unicycler>).

2.5. Bioinformatic analyses

Genomes were interrogated for their phylogroup, lineage structure, e-serotype, carriage of plasmid replicon types, and virulence and antimicrobial gene carriage. Identification of species was performed with Kraken2 v2.0.7 (Wood et al., 2019) and confirmed using mlst v2.19.0 (Jolley et al., 2018) (<https://github.com/tseemann/mlst>). Gene identification for the entire dataset was performed using ABRicate v1.0.1 (<https://github.com/tseemann/abricate>) and the following databases: ResFinder (Zankari et al., 2012), VFDB (Chen et al., 2005), PlasmidFinder (Carattoli et al., 2014). ABRicate was also utilised to identify serogroup alleles using the SerotypeFinder database (Joensen Katrine et al., 2015) and F plasmid replicon sequence types (F RST) (Carattoli et al., 2014). All aforementioned databases were accessed on 23/12/2020. Additional genotyping of reference datasets and plasmids was performed using BLASTn (Camacho et al., 2009) and the above databases. Whole genome and plasmid comparisons were performed and visualised with progressiveMauve v20150226 (Darling et al., 2010). Phylogenetic analyses involving multiple sequence types were generated using PhyloSift (Darling et al., 2014) v1.0.1 and FastTree 2 (Price et al., 2010) (specifically the double-precision version FastTreeDbl, originally accessed 29/10/2018) while phylogenetic analyses of individual sequence types and plasmid families were performed using parsnp and gingr from the Harvest Suite v1.2 (Treangen et al., 2014). All trees were visualised with iTOL (Letunic and Bork, 2019) (<https://itol.embl.de/>). Circular BLASTn alignment visualisation was performed with BRIG v0.95 (Alikhan et al., 2011) (<https://brig.sourceforge.net/>). Annotations were generated with prokka v1.14.6 (Seemann, 2014) and visualised with the SnapGene software (www.snapgene.com). Reference sequences were sourced through Enterobase (Zhou et al., 2020) (<https://enterobase.warwick.ac.uk/>). Intimin subtyping was performed using BLASTn (no cut-off values) against the alleles provided by Zhang et al. (2002). Subtypes were reported as the closest known subtype with nucleotide identity of >99 %.

The transmissible locus of stress tolerance (tLST) was detected and typed using BLASTn alignments against the following accessions: CP025739.1 (tLST1), CP061749.1 (tLST2), CP010237.1 (tLST3a) and CP061755.1 (tLST3b). tLST typing based on ORF presence/absence is described by Zhang and Yang (2022). Positive matches were defined by a minimum 95 % alignment identity and 90 % coverage of the whole locus. Suspected dual carriage was reported for isolates with coverage over 120 %.

3. Results

3.1. Collection sampling regime

In total, 431 *E. coli* genomes were sequenced from a total of 140 sampling events (swabs) spanning the entire breeding season, with 15–67 isolates per sampling date. Isolates were from a total of 69 gulls, 51 chicks hatched during the breeding season and 18 adult birds. It should be noted that this sampling strategy frequently led to the recovery of clones from individual samples, a detail that was factored into

our assessment of lineage prevalence. Information on each isolate including bird identifiers, metadata and genotyping can be found in Supplementary Table 1.

3.2. Phylogenetic distribution

The 431 *E. coli* isolates represented 123 sequence types spanning all 7 major phylogroups (Fig. 1), including: A (95 isolates; 26 STs), B1 (144 isolates; 38 STs), B2 (103 isolates; 31 STs), D (34 isolates; 15 STs), F (21 isolates; 4 STs), C (13 isolates; 2 STs), and E (21 isolates; 7 STs).

3.3. Carriage of the Yersinia High Pathogenicity Island

The *Yersinia* High Pathogenicity Island is a critically important chromosomal virulence region involved in ExPEC disease (Royer et al., 2023). The HPI was identified in 169 isolates (39%) and across six of the

seven phylogroups. Specifically, the HPI featured prominently in B2 (90/103; 87%), F (16/21; 76%), D (16/34; 47%), C (7/13; 54%) and B1 (27/144; 19%). In phylogroup B2, ST978 ($n = 11$), ST372 and ST8611 ($n = 8$ for each) and ST681 ($n = 7$) were most numerous. In phylogroup D, ST1143 and ST68 were noted carriers, while ST1671 and ST88 were carriers from phylogroup C. In the phylogroup B1, widely regarded as a commensal phylogroup (Stoppe et al., 2017; Sabaté et al., 2006), ST58 ($n = 20$) and ST162 ($n = 5$) were carriers of HPI while in phylogroup A, again a commensal group (Sabaté et al., 2006), HPI carriage was rare, found in only 13 isolates from the ST10 clonal cluster. The carriage of VAG-associated elements (HPI, F plasmids) is broken down by phylogroup in Supplementary Fig. 1.

3.4. Carriage of F virulence plasmids

Potential virulence was also assessed based on the carriage of

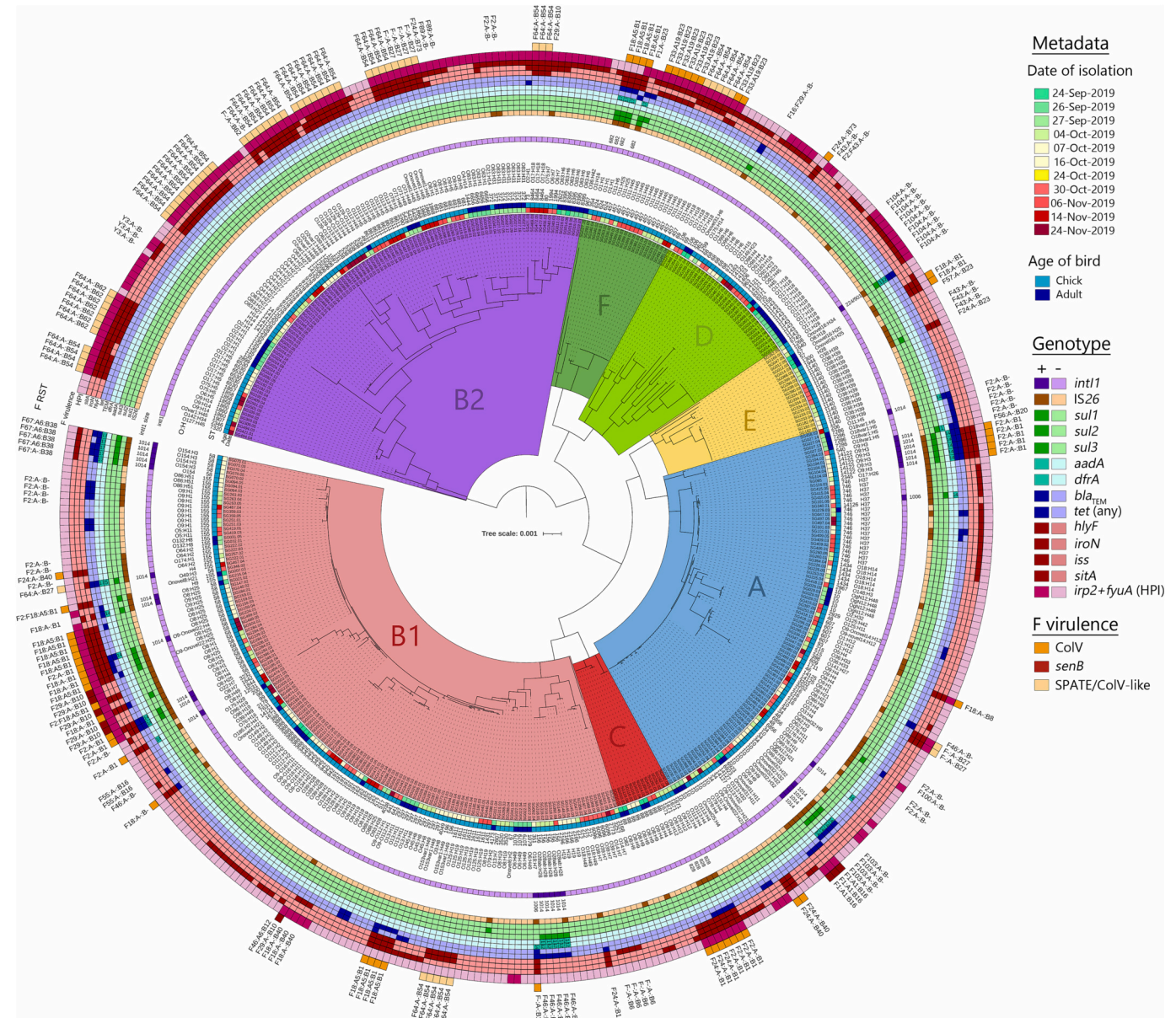


Fig. 1. A mid-point rooted maximum likelihood phylogenetic tree of *E. coli* isolates from gulls breeding on Big Island, generated using PhyloSift. Clades are coloured by phylogroup, with metadata and genotypic information for each isolate placed at each tip, including sequence type (ST), detected serotype (O:H), *int1* hit (BLASTn match size to *int1* reference) and squares indicating gene presence (darker)/absence (lighter) based on the provided key. F virulence markers are presented as either red (positive for *senB*), orange (positive for ColV) or pale orange (SPATE-ColV-like) alongside F plasmid RST data.

virulence-associated genes (VAGs) associated with key F virulence plasmids, specifically ColV plasmids and plasmids that carry *cjrABC-senB*. ColV plasmids were identified by applying a modified criteria (D. Li et al., 2023) originally defined by Liu et al. (2018). Fifty-two (12.1 %)

isolates represented by 15 sequence types met one of these criteria, of which 30 (58 %) also carried HPI. ST58, an emerging phylogroup B1 pathogen (Reid et al., 2022), was the dominant sequence type carrying ColV plasmids ($n = 13/27$ ColV+, multiple serotypes). We identified ten

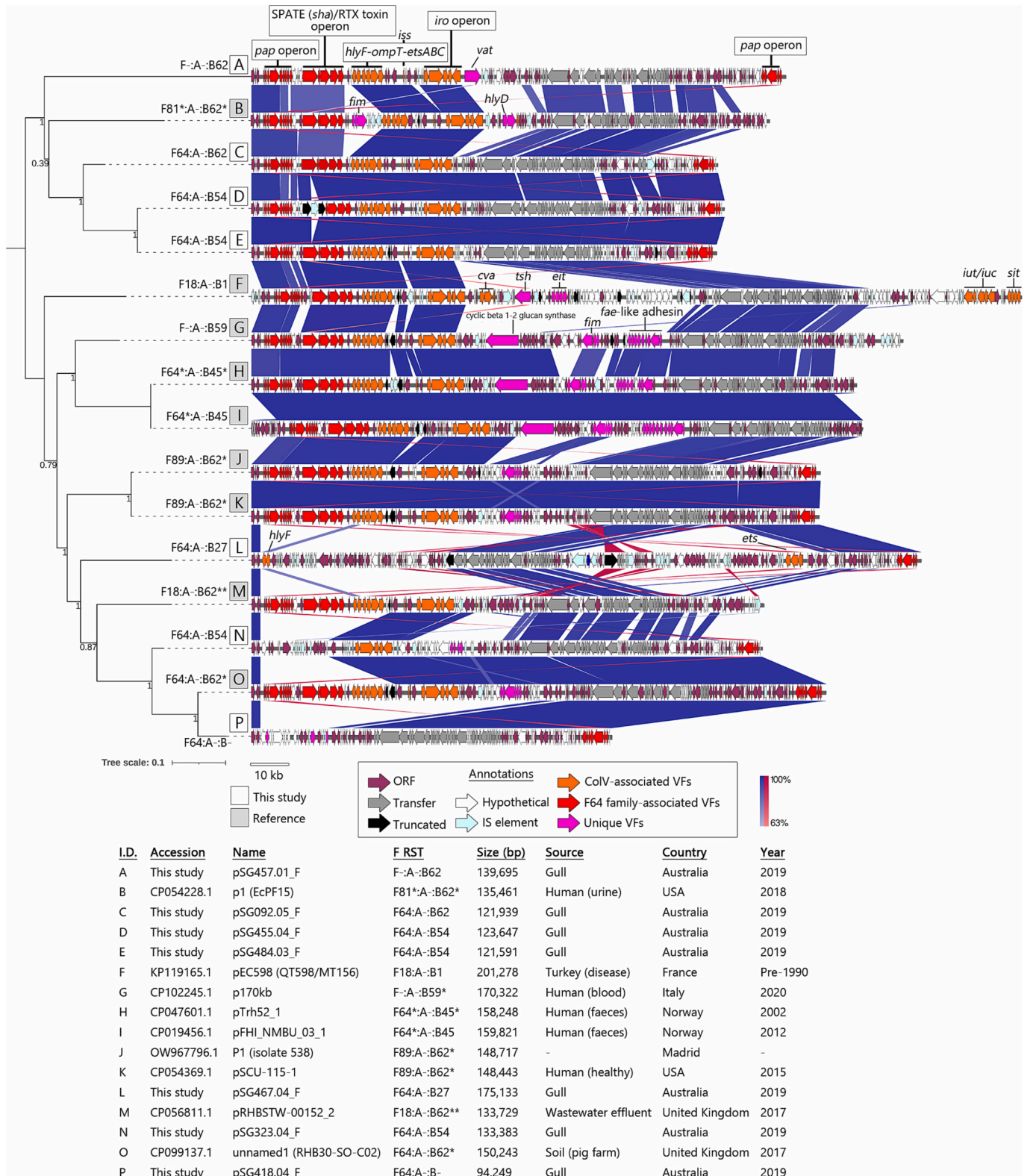


Fig. 2. Annotations and phylogenomic comparisons of complete F64/SPATE family plasmids from *E. coli* sourced from Australian silver gulls (this study) and references sequences from GenBank, including examples from human disease, healthy humans, and animal agriculture. Includes a phylogenetic analysis of conserved plasmid sequence (plasmid E, pSG484.03_F used as reference) with annotations and BLASTn alignments visualised by EasyFig between neighbouring plasmids.

F plasmid replicon sequence types (RSTs) among the 52 isolates carrying ColV F plasmids; most were F18:A5:B1 ($n = 14$), F2:A:B1 ($n = 13$) and F18:A:B1 ($n = 5$). *E. coli* that carry F virulence plasmids harbouring *cjrABC-senB* comprise diverse human ExPEC (Cummins et al., 2022). This virulence genotype was uncommon in the cohort (9/431; 2 %) and were found alongside F29:A-B10 plasmids in ST58 O8:H1 ($n = 5/5$) and ST162 O9:H19 ($n = 1/4$), and F1:A1:B16 in ST10 O9:H9 ($n = 3/3$). Notably, all 9 isolates also carried HPI. In addition, we identified 62 (14.4 %) isolates carrying plasmids (predominantly F64) that do not strictly meet defining criteria for ColV but encoded a similar virulence genotype. Notably, most (56; 90 %) of these isolates also carried the HPI.

To characterise these plasmids, complete sequences were generated using long read sequencing for seven representatives with these ColV-like genotypes: ST131 O62:H4 (B2, F64:A-B-), ST155 O-H4 (B1, F64:A-B27), ST457 O11:H45 (F, F64:A-B54), ST978 O4:H27 (B2, F64:A-B54), ST1597 O39:H4 (B2, F-A-B62), ST1868 Nov:H4 (B2, F64:A-B54) and ST6530 O17:H5 (B2, F64:A-B62). BLASTn alignments to the GenBank database identified nine plasmids related to these, at a minimum of 80 % coverage (Fig. 2). The reference plasmids were from a range of countries, times, and sources, including poultry, humans (healthy and diseased), wastewater and animal agriculture. They

encompassed multiple F RST types, including F64, F18, F81* and F89 variants, however phylogenetic analysis demonstrates these plasmids belong to a single family despite this variability. A comparative analysis, including annotation, phylogenetic analysis and BLASTn alignments performed for the sixteen plasmids (Fig. 2) revealed that most plasmids encoded a conserved virulence genotype, including *iro*, *ets*, *iss*, *hlyF* and *ompT* (all ColV-associated), plus the autotransporter *sha* as part of an RTX toxin operon, and two distinct *pap* operons. Three plasmids lacked this genotype (plasmids L, N and P in Fig. 2). While the presence of many of these genes is used to identify ColV plasmids, the organisation of these genes is distinct compared to typical F2:A-B1 ColV plasmid pSDJ2009-52F (MH195200.1). A single plasmid from this set, pEC598 (F18:A-B1; plasmid F in Fig. 2) was genotypically, a bona fide ColV plasmid, and was the only representative to include genes *cva*, *iut/iuc* and *sit*. Based on the timing of isolation of this plasmid (pre-1990, unable to confirm specific date), its phylogenetic placement and its genotype, our analysis suggests this SPATE-positive family of plasmids is a highly diverged lineage of ColV plasmids disseminating a distinct set of virulence factors. Notably, the *hlyF* gene found on these plasmids has only 80 % nucleotide identity to the variant previously observed on ColV plasmids, but interestingly this variant is the original allele investigated when *hlyF* was

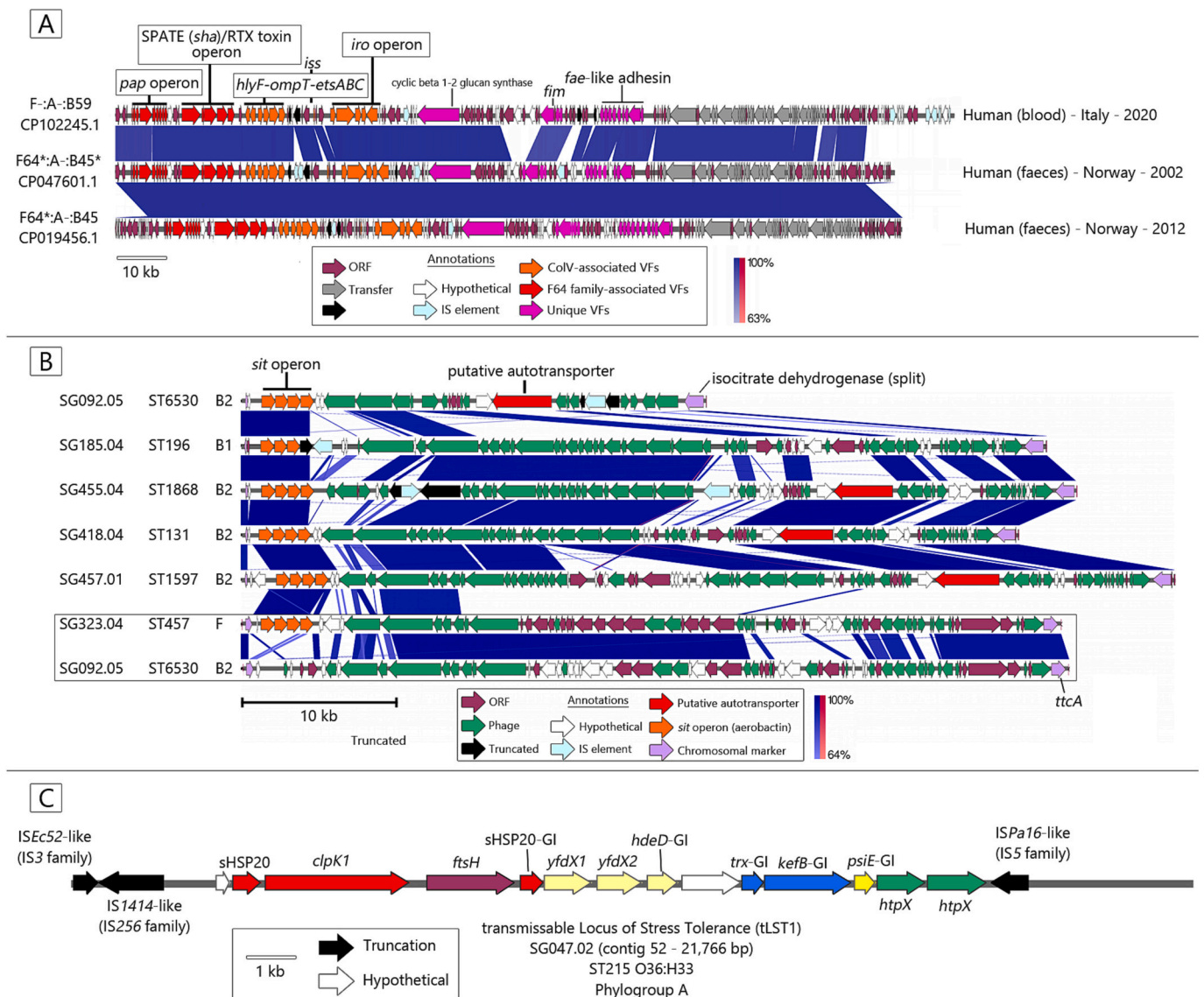


Fig. 3. Annotations and BLASTn alignments of A) notable SPATE encoding plasmids from human samples, B) bacteriophages hosting *sitABCD*, and C) transmissible locus of stress tolerance from ST215 isolate SG047.02.

first associated with avian *E. coli* by Morales et al (2004) (Morales et al., 2004). HlyF is considered an important virulence factor within uropathogenic *E. coli* through the regulation of outer membrane vesicles and predominantly associates with ColV plasmids (Murase et al., 2016). The allelic divergence of *hlyF* suggests either distinct gene origins or the dissemination of a hyper-variant *hlyF* alongside the ColV genotype. While the genotype described above was common to this family of plasmids, including a conserved contextual structure within most examples, many of the plasmids had captured additional virulence factors. These included, but were not limited to, autotransporters (*vat* and *tsh*), adhesins (*fim* and *fae*-like operons), and cyclic beta 1–2 glucan synthase, a polysaccharide virulence factor observed in *Brucella* spp. and other bacteria. Annotations and BLASTn alignments for the three plasmids encoding cyclic beta 1–2 glucan synthase, all derived from human isolates, (including sepsis) are provided in Fig. 3A.

Another distinct example from this analysis is pSG467.04_F (plasmid L in Fig. 2; F64:A-B27), which has a very altered structure likely due to the effects of multiple IS elements. This plasmid has notably lost the virulence content observed in the other plasmids, and instead captured a different *hlyF* allele (the ColV variant) and *ets*, highlighting the importance of these genes in the avian microbiome. A similar F64:A-B27 plasmid has been observed from poultry in Paraguay (Nesporova et al., 2021), indicating a potential international distribution.

A BLASTn comparison generated using BRIG was used to observe similarity between pSG484.03_F and representative whole genome sequences from our collection (Supplementary Fig. 2). The representatives included isolates hosting F64:A-B54 (nine STs), F64:A-B62 (ST6530), F64:A-B27 (ST155), F64:A-B- (ST131) and F-A-B62 (ST1597) and F-A-B27 (ST681 and ST14125). This set of alignments highlighted coverage of the plasmid backbone region and virulence region of the plasmid, although it was noted that several representatives lacked the virulence region, a resolved example of which can be seen in completed plasmid pSG418.04_F from ST131 (plasmid P in Fig. 2).

A key genetic feature of ColV plasmids, the iron and manganese transporter operon *sitABCD*, was notably lacking in the SPATE-positive plasmids in our dataset yet was identified in 164 (38 %) isolates that lacked a ColV plasmid (Fig. 1). Investigation of the *sit* operon context within the long reads described above attributed this presence to two distinct bacteriophages mobilising *sit*, with one variant also encoding a yet unidentified putative autotransporter (Fig. 3B). Even across phylogroups, these phages had conserved insertion sites – one splitting a chromosomal isocitrate dehydrogenase gene, and the other between universal stress protein F and *ttcA*. Similarities between these phages suggest homologous recombination may have played a role in the transfer of *sit*, however the presented examples demonstrate high variation in their overall structure.

3.5. Carriage of the transmissible locus of stress tolerance

The transmissible locus of stress tolerance (tLST) constitutes a chromosomally borne, mobile locus (Fig. 3C) that confers an extreme heat-resistance phenotype and greater resistance to chlorination and advanced oxidants (Yu et al., 2022; Wang et al., 2020; Mercer et al., 2017; Ma et al., 2020; Gajdosova et al., 2011), raising concerns that diverse enterobacterial populations, including *E. coli* may increasingly develop a capacity to withstand diverse physiochemical treatments central to modern wastewater treatment and food production (Guragain et al., 2021). Screening among the 431 *E. coli* genomes identified tLST in 20 isolates (7 STs; 9 lineages; Table 1), exclusively in phylogroups A and B1, and of the following subtypes: tLST1 ($n = 9$), tLST2 ($n = 7$), tLST3b ($n = 4$). Of these, 8 isolates were noted to have single carriage and 12 with suspected dual carriage, giving a total of only 4.6 % carriage in the collection. Positive isolates were separated into single hit and “dual carriage” categories, as there was clear evidence of multiple contigs providing repeated coverage of the reference locus in some isolates, although short-read assembly data was not capable of resolving any

concise examples for annotation when dual carriage was suspected. This prompted us to examine carriage of the tLST in our 2012 dataset (425 *E. coli* genomes (Wyrsh et al., 2022a)) which was derived using antibiotic selection. Of the 425 *E. coli* genomes, 60 isolates were positive for a single copy of the locus, with a further 8 isolates suspected of dual carriage, giving a total 16 % carriage across the 2012 dataset. Like the 2019 collection, tLST was identified exclusively in phylogroups A and B1, with the following subtype distribution: tLST1 ($n = 61$), tLST2 ($n = 5$), tLST3a ($n = 2$). Across both datasets, a total of 36 *E. coli* sequence type/serotype combinations were positive for the locus comprised of 30 phylogroup A lineages and 6 group B1 lineages (summarised in Table 1). Co-carriage of HPI among isolates with tLST was rare (Table 1) but co-carriage with multiple antibiotic resistance gene cargo was frequently observed in the 2012 isolates which were selected for resistance to a single clinically important antibiotic. Prominent sequence types with multiple serotype representatives were ST216 and ST1139, both from phylogroup A.

3.6. Antimicrobial resistance

Genes conferring resistance to twelve classes of antibiotic were observed in the isolates from 2019, including 27 distinct genes/alleles, with 86 isolates (20 %) hosting at least one mobilised ARG. Resistance to tetracycline was most abundant (62 isolates, 4 genes, predominantly *tetA*), followed by aminoglycosides (44 isolates, 4 genes/operons, predominantly *strAB*), penicillins (44 isolates, *bla*_{TEM} only) and sulphonamides (41 isolates, predominantly *sul2*). Phylogroup B2 isolates were notably lacking in ARG carriage (Supplementary Fig. 1), with just one ST73 isolate positive for *bla*_{TEM} and one ST8611 isolate positive for *mcr-10* the only examples of captured AMR from 103 representatives of the group.

Forty-one isolates (9.5 %) were classified as genotypically multiple-drug resistance (MDR; 3 classes or more), with the majority of these belonging to phylogroups B1 ($n = 20$, predominantly ST58) and A ($n = 14$). Most of the multiple-drug resistance was associated with a class 1 integron (33/41, 80.5 %), with 40/431 (9.3 %) isolates carrying a full or truncated copy of the class 1 integrase gene *intI1* overall. IS26, a frequent component in mobilised complex resistance structures, was observed in 35/41 (85 %) of these multi-drug resistant isolates, and in 101 isolates (23.4 %) overall, indicating that these isolates are primed to acquire resistance gene cargo. A range of truncated *intI1* genes were observed, including previously characterised truncation sizes from gulls (Wyrsh et al., 2022a) such as *intI1*_{Δ682} and *intI1*_{Δ1006}. Of the sulphonamide resistance genes observed, *sul2* ($n = 33$) followed by *sul3* ($n = 8$) and *sul1* ($n = 4$) were identified, a secondary indication that most class 1 integrons have been infiltrated, and structurally modified, by IS26. Truncations of the resistance gene *mefB*, often associated with *sul3*-type class 1 integrons (Wyrsh et al., 2022a), were predominantly *ΔmefB*₂₆₀, the most common truncated version of *mefB* seen in *sul3*-type class 1 integrons (Wyrsh et al., 2022c).

Several genes of clinical consequence were identified, though at very low numbers. A single multi-drug resistant ST457 O11:H25 isolate was the only ESBL-positive representative, encoding *bla*_{CTX-M-15} alongside *strAB* (aminoglycosides), *sul2* (sulphonamides), *floR* (phenicols), *qnrS* (fluoroquinolones) and *tetA* (tetracyclines), but no class 1 integron. Colistin resistance gene *mcr-10* was identified in two isolates, an ST2967 O148:H3 (phylogroup A) isolate and the aforementioned ST8611 O113:H5 (phylogroup B2) isolate. Neither isolate encoded any other captured ARGs (Supplementary Table 1).

3.7. Comparison to isolates selected by antibiotics circa 2012

Previous sampling to investigate the presence of antibiotic resistant *E. coli* within the silver gull in 2012 revealed widespread carriage of AMR, including multiple-drug resistance formed around class 1 integron structures and ARGs mobilised by IS26 (Wyrsh et al., 2022a). The 2012

Table 1

List of lineages (sequence type/serotype combinations) encoding the transmissible locus of stress tolerance from both 2012 (antibiotic selected) and 2019 non-selected collections. Lineages from this study are highlighted in grey. Lineages denoted with a Y in Dual Carriage had BLASTn coverage exceeding 120 % (range 120–240 %) of the locus across multiple contigs. Virulence and integron counts are provided for cases where not all isolates from that lineage were positive for the gene or element.

Group	ST	Serotype	Count	Year	tLST subtype (dual carriage)	Site	Virulence (n)	Integrans (n)	Critical ARGs
B1	58	O100/O154:HNT	8	2012	1	Five Islands	–	<i>int1</i> (2), <i>int1</i> _{Δ919} (6), IS26	<i>bla</i> _{IMP-4} , <i>bla</i> _{OXA-1} , <i>bla</i> _{SHV-12}
A	189	O124/O164:H45	2	2012	1	Five Islands	–	<i>int1</i> , IS26	<i>bla</i> _{IMP-4}
A	215	O36:H33	2	2019	1	Five Islands	–	–	–
A	216	O3:H4	3	2019	3b (Y)	Five Islands	–	IS26	–
A	216	O154:H4	8	2012	1	Five Islands	HPI (1)	<i>int1</i> (1), <i>int1</i> _{Δ931} (1), <i>int1</i> _{Δ919} (3), <i>int1</i> _{Δ899} (3), IS26 (7)	<i>bla</i> _{IMP-4} , <i>bla</i> _{OXA-1} , <i>bla</i> _{CTX-M-24} , <i>qnrS1</i>
A	216	O19:H4	2	2012	1	Five Islands	–	<i>int1</i> _{Δ931} , IS26	<i>bla</i> _{IMP-4} , <i>bla</i> _{OXA-1} , <i>bla</i> _{SHV-12} , <i>qnrA1</i>
A	216	O36:H27	6	2012	1, 2 (Y)	Five Islands	–	<i>int1</i> (2), <i>int1</i> _{Δ761} (4), IS26	<i>bla</i> _{IMP-4} , <i>bla</i> _{SHV-12} , <i>qnrA1</i>
A	216	O36:H54	1	2012	2 (Y)	Five Islands	–	<i>int1</i> , IS26	<i>bla</i> _{IMP-4} , <i>bla</i> _{SHV-12} , <i>qnrA1</i>
A	216	O45:HNT	2	2012	1 (Y)	Five Islands	–	<i>int1</i> _{Δ923} , IS26	<i>bla</i> _{IMP-4} , <i>bla</i> _{OXA-1} , <i>bla</i> _{SHV-12} , <i>qnrS1</i>
A	216	O86:H4	1	2012	1	Five Islands	–	<i>int1</i> , IS26	<i>qnrS1</i>
A	216	O86:H9	1	2019	2 (Y)	Five Islands	–	–	–
B1	224	O8:H23	1	2012	1	Five Islands	–	<i>int1</i> _{Δ899} , IS26	<i>bla</i> _{IMP-4} , <i>bla</i> _{OXA-1} , <i>bla</i> _{CTX-M-15} , <i>qnrS1</i>
B1	345	O8/O134*:H21	1	2012	1	Five Islands	–	<i>int1</i> _{Δ899} , IS26	<i>bla</i> _{IMP-4} , <i>bla</i> _{OXA-1}
A	398	O8/O155:H20	1	2012	1	White Bay	–	<i>int1</i> , IS26	<i>bla</i> _{CTX-M-15} , <i>qnrS1</i>
A	541	O148:H40	1	2012	1	Five Islands	–	<i>int1</i> , IS26	<i>bla</i> _{IMP-4} , <i>qnrA1</i>
A	542	O109:H45	1	2012	1	Five Islands	–	<i>int1</i> _{Δ931} , IS26	<i>bla</i> _{IMP-4} , <i>bla</i> _{OXA-1} , <i>bla</i> _{SHV-12} , <i>bla</i> _{CMY-2}
A	607	O1:H12	3	2019	2 (Y)	Five Islands	–	IS26	–
A	607	O9:H12	2	2019	2 (Y)	Five Islands	–	–	–
A	744	O89*/O162:H25	1	2012	1	Five Islands	–	<i>int1</i> _{Δ899} , IS26	<i>bla</i> _{IMP-4} , <i>bla</i> _{OXA-1} , <i>bla</i> _{CMY-2}
A	1114	O10:H26	2	2012	1	Five Islands	–	<i>int1</i> , IS26	<i>bla</i> _{IMP-4}
A	1139	O157:H10	4	2012	1	Five Islands	–	<i>int1</i> _{Δ931} , IS26	<i>bla</i> _{IMP-4} , <i>bla</i> _{OXA-1} , <i>bla</i> _{SHV-12} , <i>qnrA1</i>
A	1139	O5:HNT	14	2012	1	Five Islands	–	<i>int1</i> _{Δ931} , IS26	<i>bla</i> _{IMP-4} , <i>bla</i> _{OXA-1} , <i>bla</i> _{SHV-12} , <i>qnrA1</i>
A	1139	O8:HNT	1	2012	1	Five Islands	–	–	<i>bla</i> _{CTX-M-15}
A	1139	O9:H20	1	2012	1	Five	–	<i>int1</i> _{Δ931} , IS26	<i>bla</i> _{IMP-4} , <i>bla</i> _{OXA-}

						Islands			1, <i>bla</i> _{SHV-12} , <i>qnrB2</i>
A	1421	O9:H4	1	2012	1	Five Islands	–	<i>int1</i> _{Δ899} , IS26	<i>bla</i> _{IMP-4} , <i>bla</i> _{OXA-1} , <i>bla</i> _{CMY-2} , <i>bla</i> _{CARB-2}
A	1434	O18:H14	5	2019	1	Five Islands	–	–	–
A	2967	O148:H3	1	2019	2 (Y)	Five Islands	–	IS26	<i>mcr-10</i>
B1	3168	O82:HNT	1	2019	3b (Y)	Five Islands	–	IS26	–
A	3202	O8:H21	2	2019	1 (Y)	Five Islands	–	–	–
B1	4657	O93:H7	3	2012	1, 3a (Y)	Five Islands	–	<i>int1</i> (2), <i>int1</i> _{Δ931} (1), IS26	<i>bla</i> _{IMP-4} , <i>bla</i> _{OXA-1} , <i>bla</i> _{SHV-12} , <i>qnrB2</i>
A	4658	O28ab:H37	1	2012	1	Five Islands	–	<i>int1</i> _{Δ899} , IS26	<i>bla</i> _{IMP-4} , <i>bla</i> _{OXA-1} , <i>bla</i> _{CTX-M-14}
A	4658	ONT:H37	1	2012	1	Five Islands	ColV	<i>int1</i> , IS26	<i>bla</i> _{IMP-4} , <i>bla</i> _{CTX-M-14}
A	6932	O154:H4	1	2012	1	White Bay	–	–	<i>bla</i> _{CMY-2}
A	8763	O51:H9	2	2012	1	Five Islands	HPI	<i>int1</i> _{Δ919} , IS26	<i>bla</i> _{IMP-4} , <i>bla</i> _{OXA-1} , <i>bla</i> _{CTX-M-15} , <i>qnrB1</i>
B1	12547	O86:H51	1	2012	1 (Y)	Five Islands	–	<i>int1</i> _{Δ931} , IS26	<i>bla</i> _{IMP-4} , <i>bla</i> _{OXA-1}

dataset was comprised of 424 isolates collected from 323 bird samples, selected on media supplemented with either meropenem (carbapenem resistance), cefotaxime (ESBL) or ciprofloxacin (fluoroquinolone resistance), resulting in a similar number of isolates and similar sequence type diversity to the current study. However, the distribution of isolates within phylogroups is profoundly different between the 2012 and 2019 datasets (Fig. 4). In the 2019 non-selective study, more B1 and B2

lineages were observed, as well as fewer isolates in groups A, D and F. Given the general lack of AMR associated genes and elements (namely IS26) found within the B1 and B2 isolates from 2019 (Fig. 1), this is perhaps expected and simultaneously, highlights phylogroup A lineages as the predominant carriers of AMR in this comparison (Supplementary Fig. 1). Despite the differences in isolation protocol, common sequence types included ST457, ST10, ST746 and ST58, albeit with multiple

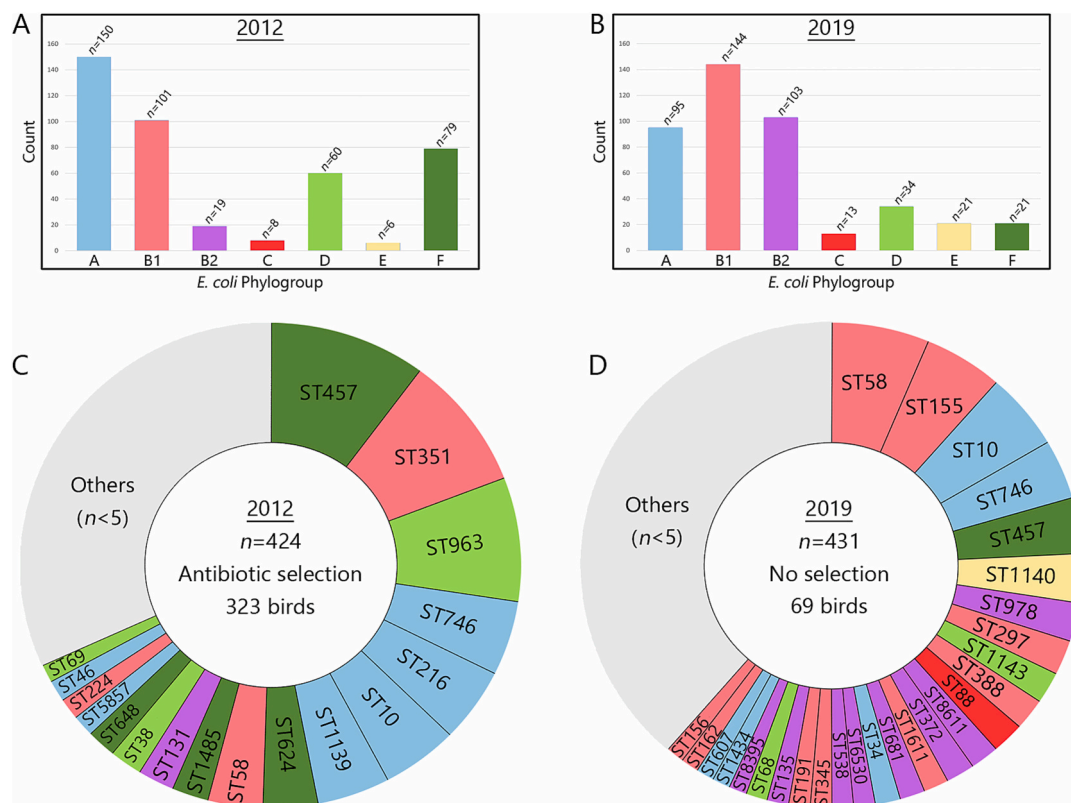


Fig. 4. Phylogroups and sequence types identified in *Escherichia coli* collections sampled in 2012 (A/C) and 2019 (B/D). Sequence types have been ordered by count of isolates and are colour coded by phylogroup. Any sequence type with fewer than five isolates was grouped into “Others”. Total number of isolates from each phylogroup in parts A and C are represented as “n = X” at the top of each column.

identified lineages coupled with distinct genotypes within each sequence type.

Combining isolates from 2012 and 2019 into a single phylogenetic tree illustrates the broad spectrum of *E. coli* isolates to be found in the Australian silver gull (Fig. 5). Twenty clades were identified that include isolates from both studies, with their predominant (and sometimes exclusive) sequence types labelled in Fig. 5. From these twenty clades, eight sequence types included isolates of the same serogroup from both 2012 and 2019 collections, including some of the more well represented sequence types such as ST457, ST351 and ST746.

To detail the relationships between some of the most closely related

isolates from 2012 and 2019, single nucleotide variant (SNV) counts were generated for ST372, ST624 and ST1140, selected as they shared potentially matching lineages based on serotype and genotype. In the case of ST372, two subclades were formed in the initial PhyloSift analysis, one comprised entirely of 2019 isolates, and one comprised of three isolates from 2012 and one from 2019. This latter group was separated by only 81–114 SNVs. Isolates from ST624 were also closely related, with the distance between isolates ranging from 91 to 138 SNVs across three isolates from 2012 and fifteen from 2019. This data is also reflected in the genotypes of these isolates, with all ST624 encoding the *intI1*_{Δ682} truncation and an F18:A5:B1 ColV plasmid. The closest

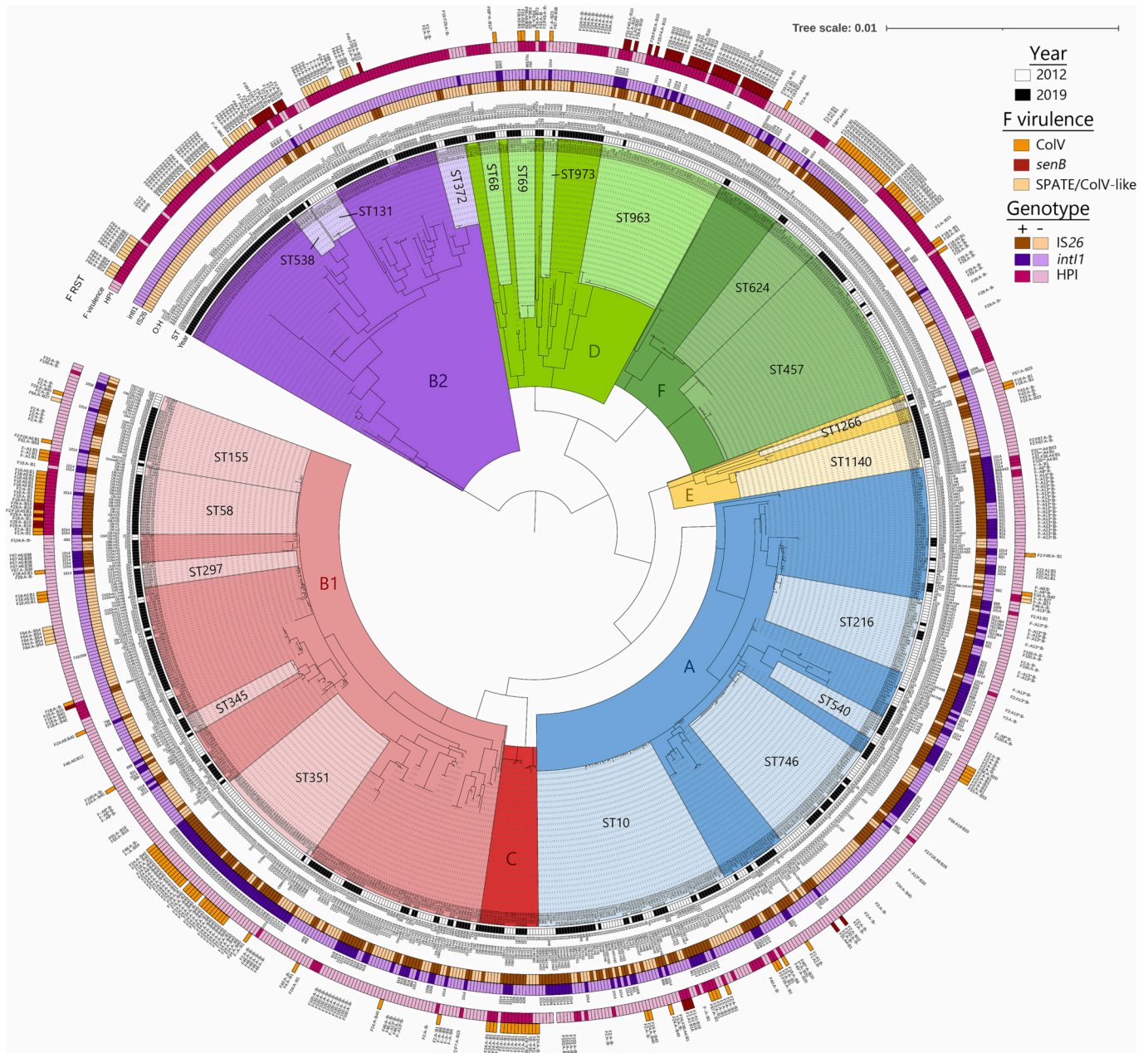


Fig. 5. A mid-point rooted maximum likelihood phylogenetic tree of *E. coli* isolates collected from coastal New South Wales but predominantly from the Big Island breeding colony of silver gulls in this study (2019) and a study using antibiotic selective media in 2012, generated through PhyloSift. Clades are coloured by phylogroup, with metadata and genotypic information for each isolate placed at each tip. Highlighted subclades show sequence types that were sourced from both 2012 and 2019 collections. Data includes sequence type (ST), detected serotype (O:H), *intI1* hit (BLASTn match size to *intI1* reference) and squares indicating gene presence/absence, where darker colours indicate positive detection. Genes included are IS26, *intI1* and *irp2* (representing the Yersinia HPI). Virulence markers are presented as either red (positive for *senB*) or orange (positive for ColV) alongside their relevant F plasmid RST data. Isolates from the current study are named as “SG”, while isolates from the previous study are named based on antibiotic selection, as “CE” (cefotaxime), “m1” (meropenem) or “H” (ciprofloxacin).

relationships from these analyses are summarised in Supplementary Table 2.

3.8. Notable lineages

Isolates that carried the HPI, an F virulence plasmid, and ARGs represent critical epidemiological targets for the tracking of potential pathogens in wildlife. Outside of phylogroup B2 (described below), the most notable sequence type identified here, factoring in prevalence, VAG and ARG carriage, was ST58 ($n = 27$ isolates), in phylogroup B1. Other B1 lineages hosting ColV plasmids included ST297 ($n = 4$) and ST155 ($n = 2$), but neither carried HPI nor were MDR.

Multiple lineages of ST58 were identified, with carriage of ColV plasmids of subtypes F18:A5:B1, F18:A:B1, and F2:A:B1 observed in isolates of serogroups O8:H25, O9:H25 and O9:H4 ($n = 13$ in total). Of these, seven were considered genotypically MDR (multiple profiles but consistently including *sul2* and *strAB*) while the remaining six encoded no AMR outside a single *bla*_{TEM}. Concerningly, ST58 O8:H1 isolates ($n = 5$) were observed hosting pUTI89-like plasmids of subtype F29:A:B10 with carriage of *cjrABC-senB*, but hosted no ARGs. The majority of ST58 isolates (20/27), primarily those carrying virulence plasmids, were also positive for the HPI, demonstrating the accumulation of key virulence effectors within this emerging sequence type (Royer et al., 2023; Reid et al., 2022).

Other key lineages with recognised ExPEC virulence gene cargo included: ST88 (ColV, F24:A:B1 and HPI+; $n = 3$ isolates) and ST1671 (ColV, F2:A:B1 and HPI+; $n = 4$ isolates) from phylogroup C; ST10 O9:H9 (*cjrABC-senB*-positive, F1:A1:B16 and HPI; $n = 3$ isolates) and ST14122 (ColV, F2:A:B1 and HPI; $n = 4$ isolates) from phylogroup A; ST624 (ColV, F18:A5:B1 but no HPI; $n = 3$ isolates) and ST457 (ColV, F33:A19:B23 and HPI; $n = 8$ isolates) from phylogroup F.

Seventeen isolates, representing eight different lineages from phylogroups A (ST10; $n = 1$), B1 (ST517, ST2166; $n = 6$) and B2 (ST1907, ST2346, ST5428, ST7320, ST12596; $n = 10$), were host to multiple subtypes of intimin (*eae*), an attaching and effacing adhesin found in enteropathogenic *E. coli* (EPEC) and enterohaemorrhagic *E. coli* (EHEC). The absence of bundle-forming pilus and shiga toxin genes indicates that these isolates are atypical EPEC. Six different intimin subtypes were detected (Supplementary Table 1). None of these isolates encoded any ARGs or ExPEC virulence factors.

Remarkable diversity was observed among the 103 *E. coli* isolates residing in phylogroup B2. As expected for phylogroup B2 lineages, most isolates carried substantial virulence gene cargo including HPI (90/104; 87%) and intimin (10/13 that do not carry HPI). The top seven sequence types by frequency of isolation were ST978 (11 isolates; all O4:H27), ST8611 (8 isolates; all O113:H5), ST372 (8 isolates; 7 O83:H31), ST538 (7 isolates, O129-O13:H4), ST681 (7 isolates; mixed serotypes), ST135 (6 isolates; all O2:H1) and ST6530 (6 isolates; all O17:H5). One single ST131 O62:H4 isolate was recovered, a rare serogroup for ST131, with only seven representatives currently available in Enterobase. Of these sequence types, all except ST8611 and ST6530 have previously been identified in ExPEC causing sporadic or persistent urinary tract and blood stream infections (Hertz et al., 2016; Banerjee et al., 2013; Rodríguez et al., 2021). Carriage of ColV-associated VAGs coincided with the presence of a range of *iucA* plasmids, including genes *iroN*, *hlyF* and *sitA* but notably lacking *iucA/iut*. However, no bona fide ColV plasmids or *senB*+ isolates were recovered from the B2 clade. Across the phylogroup, IS26 was observed only in two ST372 and an ST80 isolate.

3.9. Phylogenomics through a One Health lens

From our analyses, we identified both putative ExPEC and aEPEC pathogens and lineages that are adept are persistently colonising the silver gull population. In order to perform broader phylogenomic analyses to explore potential interhost transmission events or evidence of strain sharing with other environments (e.g. humans and companion

animals) we selected three sequence types: ST58 (B1) and ST457 (F) as ExPEC, and ST746 (A) as an established commensal, that were represented in both the 2012 and 2019 collections. As the number of ST58 sequences available on Enterobase is high, that analysis specifically was limited to Australian isolates. Similarly, the range and number of ARGs identified across these sequence types was extensive, so this data has been made available in Supplementary Table 3.

ST58 isolates from gulls encoded a range of ExPEC virulence content, including both pUTI89-like and ColV-like plasmids and were the most notable carrier of the Yersinia HPI from phylogroup B1. Because of this variability, we sought to explore the carriage of these elements in ST58 on a national level. In this case, a phylogenetic and genotypic analysis was performed between isolates from this collection and all Australian ST58 isolates from Enterobase ($n = 88$) that afforded appropriate metadata, which included isolates from the 2012 sampling (Fig. 6). Approximately half of the included Australian ST58 ($n = 57$, 64.7%) formed a subclade (highlighted in light red in Fig. 6) with significant HPI and F virulence plasmids carriage. Several instances of highly related strains appearing across diverse source hosts were noted, including three separate clusters of isolates linking gulls to companion animals (Fig. 6, Table 2). A particularly close cluster of O9:H4 isolates shared between canines and gulls gave counts of 26–74 SNVs. Several pairs of ST58 isolates shared between gulls and wild ibis are indicative of bacterial transfer between wild avian species. Overall, the potential for carriage of AMR markers in Australian ST58 was high, with IS26 in 78 (69%) isolates and *intI1* in 51 (45%) isolates, and an average of 3.7 ARGs identified per isolate at a range 0–14 across 36 different ARG genes/alleles (Supplementary Table 3). A total of 69/113 (61.1%) Australian ST58 isolates carried at least one ARG. Class 1 integrons hosting *sul2* ($n = 36$, 31.9%) appeared to be most prevalent.

To explore a key host of the HPI and virulence plasmids from phylogroup F, we performed a similar phylogenomic analysis of ST457, utilising 328 additional isolates from Enterobase (Fig. 7). The tree resolved five primary clades, represented by the serogroups O11:H25, O11:H45 and O11:H6. Interestingly, the dominant ST457 serogroup O11:H25 was separated into three distinct clades. Consistent HPI carriage was observed in four of those five clades. There was considerable ColV plasmid carriage across the entire sequence type ($n = 129$, 37.8%), with a spectrum of F RSTs including multiple subtypes of F2, F4, F18, F24, F33, F40 and F64. Just two of the included ST457 isolates hosted pUTI89 and were encoding *cjrABC-senB*. Class 1 integron carriage was high across ST457, with 168/341 (49.3%) isolates *intI1* positive and 150/341 (44%) carrying IS26. A total of 74 ARG genes/alleles were identified across the sequence type, with 288/341 (84.5%) isolates positive for at least one ARG. Average ARG carriage rate was 4 genes per isolate at a range of 0–22.

Two clades were demonstrative of shared human-animal colonisation. One, a clade comprised of Australian O11:H45 isolates from both gulls (2012 and 2019) and human samples (2012–2015) (highlighted red in Fig. 7), was closely related at 33–46 SNVs. A second group of Australian gull and human isolates (located in the clade highlighted green in Fig. 7) shared F1:A:B23 and *intI1*_{Δ648} genotypes, linking an isolate from gulls in 2019 to multiple human isolates from 2018 to 2020 at 24–40 SNVs.

ST746 was one of the most abundant sequence types in our collections (17 isolates from 2019 and 21 from 2012) but encoded few virulence factors. As above, a comparative phylogeny was generated against 222 references. Unlike the previous examples, all gull isolates from this collection were placed into a single clade, highlighted light blue in Fig. 8. In the case of ST746, no isolates from this study had any apparent One Health consideration, clustering only with isolates sourced from gulls in 2012. Interestingly however, there were several clades of ST746 that were predominantly from human sources and frequently encoded the HPI. Within this group, a series of O11:H19 isolates (highlighted in red in Fig. 8) each showed carriage of *cjrABC-senB* in association with F17:A:B- plasmids at a distance of 81–147 SNVs, suggesting an

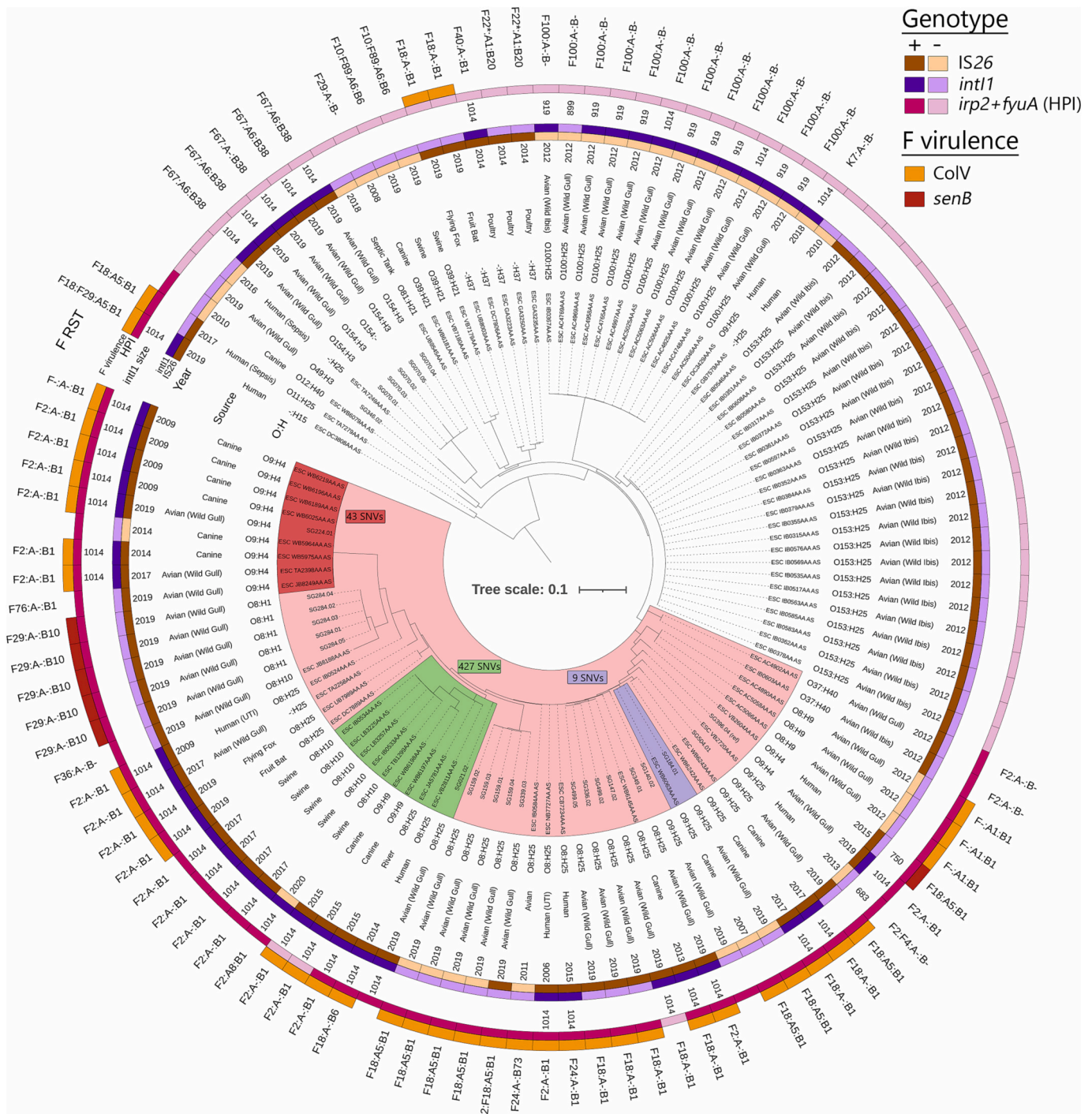


Fig. 6. A mid-point rooted maximum likelihood phylogenetic tree of 113 *E. coli* ST58 isolates from this study and Australian reference *E. coli* isolates, generated by Parsnp based on 26,523 identified variant sites. Reference sequences and metadata were sourced from Enterobase. Data includes isolate source and year, detected serotype (O:H), *int1* hit (BLASTn match size to *int1* reference) and squares indicating gene presence/absence, where darker colours indicate positive detection for labelled genes and virulence markers. Colour-coded maximum SNV counts of selected subclades are included to demonstrate scale.

internationally distributed pathogenic lineage of ST746 is in circulation. IS26 was identified in 128/236 (54.2 %) isolates and 88 (37.2 %) carry the class 1 integrase gene. ARGs were identified in 169/236 (71.6 %) ST746 isolates, with 69 genes/alleles identified at an average carriage rate of 3.4 ARGs per isolate (range of 0–17).

4. Discussion

Whole genome sequencing provided phylogenetic and genotypic

insights into *E. coli* sourced from the Australian Silver gull without antibiotic selection. The analysis resulted in the characterisation of 431 isolates representing all seven major *E. coli* phylogroups, including a diverse set of unusual group B2 lineages with extensive virulence cargo, a factor rarely investigated in wildlife (Lagerstrom and Hadly, 2021). Critically, these B2 lineages were not observed when isolation was performed using antibiotic selection as part of an extensive sampling protocol undertaken in 2012 (Wyrsh et al., 2022a). When comparing isolates from our 2012 study, where *E. coli* were isolated using

Table 2

Details of isolate clusters (~100 SNVs or less) identified during phylogenetic analyses of gull and publicly available genomes from ST372, ST624, ST58 (Australian only), ST457 and ST746. Each cluster has a specified reference isolate (Ref) with related isolates then ordered by SNV count. Isolates from this study can be identified by the "SG" identifier.

ST	Isolate	SNVs	Serogroup	Source	Country	Year	Virulence	F plasmid	<i>intI1</i> (bp)	
ST372	SG041.04	Ref	O21:H14	Gull	Australia	2019	HPI	–	–	
	CE1562	81	O21:H14	Gull	Australia	2012	HPI	–	–	
	CE1575	84	O21:H14	Gull	Australia	2012	HPI	–	–	
	CE1725	114	O21:H14	Gull	Australia	2012	HPI	–	–	
ST624	SG340.04	Ref	O1:H1	Gull	Australia	2019	ColV	F18:A5:B1	682	
	CE1938_B	91	O1:H1	Gull	Australia	2012	ColV	F18:A5:B1	682	
ST58	SG224.01	Ref	O9:H4	Gull	Australia	2019	ColV, HPI	F2:A-B1	1014	
	ESC_WB6025AA_AS	26	O9:H4	Canine	Australia	2009	ColV, HPI	F2:A-B1	1014	
	ESC_WB5975AA_AS	45	O9:H4	Canine	Australia	2014	ColV, HPI	F2:A-B1	1014	
	ESC_WB5964AA_AS	46	O9:H4	Canine	Australia	2014	HPI	–	–	
	ESC_TA2398AA_AS	51	O9:H4	Gull	Australia	2017	ColV, HPI	F2:A-B1	1014	
	ESC_JB8249AA_AS	74	O9:H4	Gull	Australia	2019	HPI	F76:A-B1	–	
ST58	SG147.02	Ref	O8:H25	Gull	Australia	2019	–	F18:A-B1	1014	
	ESC_WB6145AA_AS	44	O8:H25	Canine	Australia	2013	ColV, HPI	F18:A-B1	1014	
ST58	SG499.02	86	O8:H25	Gull	Australia	2019	ColV, HPI	F18:A-B1	–	
	SG184.01	Ref	O9:H25	Gull	Australia	2019	ColV, HPI	F18:A5:B1	–	
ST58	ESC_WB6063AA_AS	63	O9:H25	Canine	Australia	2007	ColV, HPI	F18:A5:B1	–	
	ESC_AC4902AA_AS	Ref	O37:H40	Gull	Australia	2012	HPI	F2:A-B-	–	
ST58	ESC_IB0603AA_AS	0	O37:H40	Ibis	Australia	2012	HPI	F2:A-B-	–	
	ESC_GB7579AA_AS	Ref	O-H25	Human	Australia	2010	–	–	–	
ST58	ESC_IB0546AA_AS	182	O153:H25	Ibis	Australia	2012	–	–	–	
	ESC_IB0367AA_AS	Ref	O100:H25	Ibis	Australia	2012	–	F100:A-B-	919	
ST457	ESC_AC4969AA_AS	19	O100:H25	Gull	Australia	2012	–	F100:A-B-	919	
	ESC_KB8502AA_AS	Ref	O11:H25	Human	Cambodia	2016	HPI	F2:A-B10	749	
ST457	ESC_WB9172AA_AS	47	O11:H25	Human	USA	2019	<i>senB</i> , HPI	F29:A-B10	–	
	ESC_YB2524AA_AS	51	O11:H25	Human	Singapore	2015	HPI	F2:A-B10	749	
	ESC_GB8791AA_AS	54	O11:H25	Human	Laos	2015	HPI	F2:A-B10	749	
	SG336.03	Ref	O11:H25	Gull	Australia	2019	HPI	F1:A-B23	682	
	ESC_DC3527AA_AS	24	O-H25	Human	Australia	2018	HPI	F1:A-B23	682	
	ESC_DC3472AA_AS	28	O-H25	Human	Australia	2018	HPI	F1:A-B23	682	
ST457	ESC_DC4575AA_AS	36	O-H25	Human	Australia	2020	HPI	F1:A-B23	682	
	ESC_DC3517AA_AS	38	O-H25	Human	Australia	2019	HPI	F1:A-B23	682	
	ESC_DC3674AA_AS	38	O-H25	Human	Australia	2019	HPI	F1:A-B23	682	
	ESC_DC3739AA_AS	38	O-H25	Human	Australia	2019	HPI	F1:A-B23	682	
	ESC_DC3609AA_AS	40	O-H25	Human	Australia	2019	HPI	F1:A-B23	682	
	ESC_DC8669AA_AS	Ref	O11:H6	Water/River	Japan	2013	ColV, HPI	F18:A-B-	1014	
	ESC_QA7284AA_AS	116	O11:H6	Human	Japan	2015	<i>senB</i> , HPI	F29:A-B10	–	
	ESC_MB8277AA_AS	135	O11:H6	Avian	Brazil	2019	ColV, HPI	F24:A-B1	985	
	ST457	SG053.02	Ref	O11:H6	Gull	Australia	2019	ColV, HPI	F18:A5:B1	–
		ESC_VB0021AA_AS	46	O11:H6	Poultry	Lebanon	2018	ColV, HPI	F18:A5:B1	1014
ESC_VB1387AA_AS		49	O11:H6	Wastewater - poultry	Germany	2020	ColV, HPI	F18:A5:B1	798	
ESC_QA5364AA_AS		63	O-H6	Human	Japan	2015	ColV, HPI	F2:A-B1	1014	
SG491.05		Ref	O11:H45	Gull	Australia	2019	ColV, HPI	F33:A19:B23	–	
ESC_VB2636AA_AS		33	O11:H45	Human	Australia	2015	HPI	–	–	
ST457	ESC_LB5037AA_AS	34	O11:H45	Gull	Australia	2012	HPI	–	–	
	ESC_WA5506AA_AS	34	O11:H45	Human	Australia	2014	HPI	–	–	
	ESC_VB2670AA_AS	44	O11:H45	Human	Australia	2014	HPI	–	–	
	ESC_WA5541AA_AS	46	O-H45	Human	Australia	2013	HPI	F82:A-B-	–	
	ESC_IA0789AA_AS	94	O11:H45	Human	Australia	2008	HPI	–	–	
	ESC_GA0711AA_AS	99	O11:H45	Wastewater	USA	2014	HPI	–	–	
	ESC_IA1962AA_AS	Ref	O11:H25	Currawong	Australia	2001	HPI	–	–	
	ESC_WA5552AA_AS	84	O-H25	Human	Australia	2015	HPI	–	–	
ST746	ESC_WA5530AA_AS	107	O11:H25	Human	Australia	2013	HPI	F89:A-B62	–	
	SG409.05	Ref	O-H37	Gull	Australia	2019	–	–	–	
	ESC_AC4777AA_AS	13	O-H37	Gull	Australia	2012	–	F16:A-B-	–	

antimicrobial selection, with isolates in the current study, the level of sequence type diversity remained similar, although there were marked differences in the specific lineages isolated. When no antibiotic selection was applied, we observed 123 sequence types, compared to 96 sequence types recorded in 2012 (Wyrsh et al., 2022a; Dolejska et al., 2016). This is a remarkable observation given that only 69 birds from a single breeding colony were sampled in the 2019 study (140 cloacal samples), compared to 323 birds (504 cloacal samples) sampled at three breeding colonies spanning >300 km of coastline in New South Wales, Australia in the 2012 study. While 34 sequence types across six of seven phylogroups were shared between 2012 and 2019, most displayed different serotypes and mobilised gene content, an indication of the diversity in *E. coli* that colonise wild birds living near human populations.

The number of phylogroup B2 lineages was much higher in the 2019 sampling (31 STs vs 7 STs in 2012) and numerous rare sequence types were identified. *E. coli* that belong to the B2 group feature prominently in the top 20 pandemic ExPEC sequence types (Manges et al., 2019) and are the most consistent carriers of the *Yersinia* High Pathogenicity Island (Schubert et al., 2002; Clermont et al., 2001) alongside other virulence associated genes. The lack of B2 isolates observed when antibiotic selection was applied (2012 samples), and lack of ARGs and relevant mobile genetic elements (MGEs) among the diverse B2 isolates from this study, serve as an indication that antimicrobial resistance has not infiltrated many B2 lineages carried by the Australian silver gull. While the 2012 sampling with antibiotic selection resulted in MDR *E. coli* being observed from seven phylogroups, ARGs and resistance associated MGEs

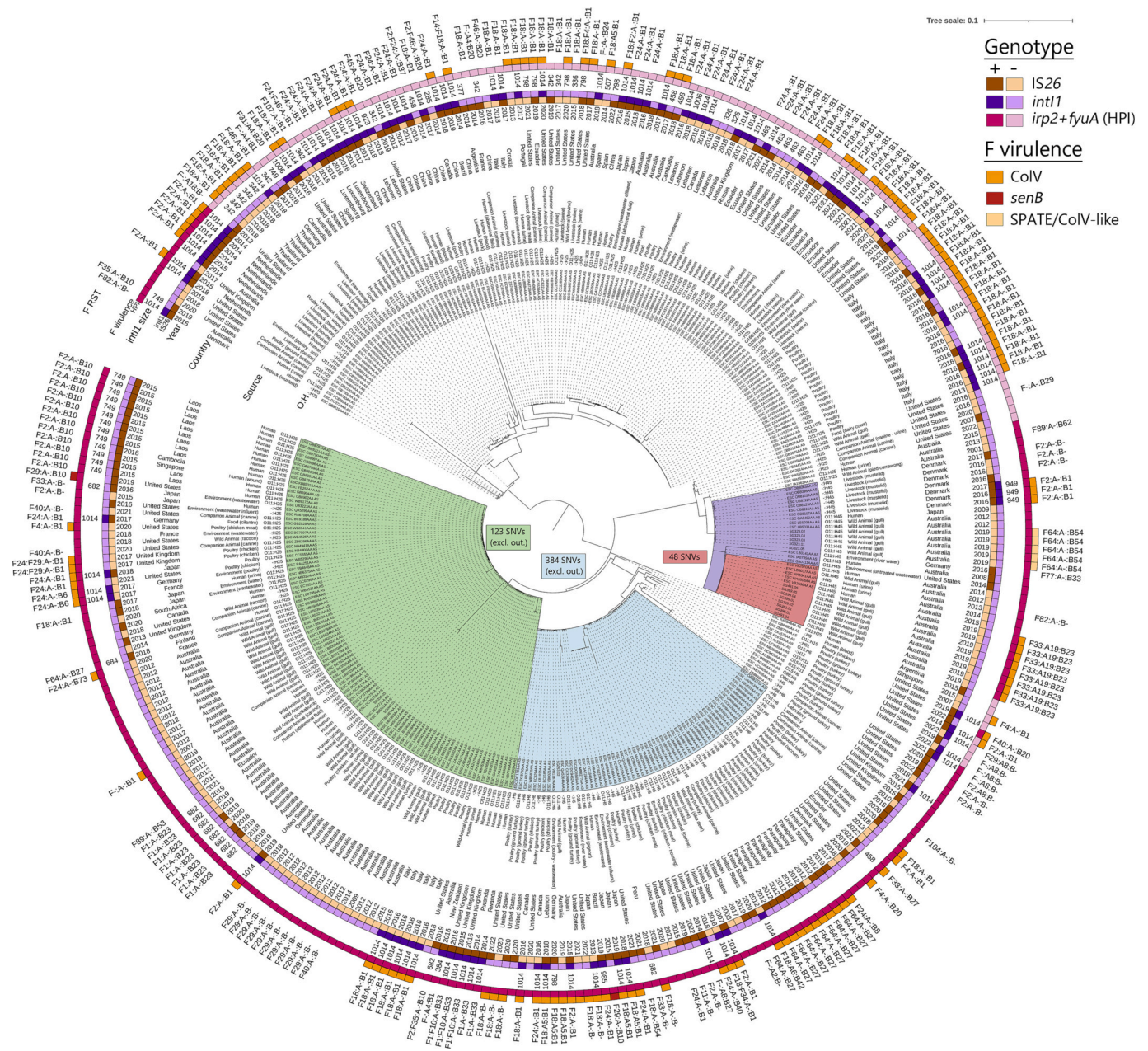


Fig. 7. A mid-point rooted maximum likelihood phylogenetic tree of 341 *E. coli* ST457 isolates from this study and reference isolates, generated by Parsnp based on 38,099 identified variant sites. Reference sequences and metadata were sourced from Enterobase. Data includes isolate source and year, detected serotype (O:H), *intI1* hit (BLASTn match size to *intI1* reference) and squares indicating gene presence/absence, where darker colours indicate positive detection for labelled genes and virulence markers. Colour-coded maximum SNV counts of selected subclades are included, with counts generated after excluding outliers (denoted by “excl. out.”).

were predominantly observed in phylogroups A, B1, C and F when no selection was applied. This included resistance to twelve classes of antibiotic, with most ARGs observed alongside the class 1 integron, although cases of *bla*_{TEM} and *tet* mobilisation by IS26 were suspected based on genotype. In the isolates from 2019, IS26 had a larger presence than the ARGs themselves, an indication that many putatively susceptible isolates were primed to acquire ARGs (Harmer et al., 2014).

Despite the phylogenetic diversity across the two collections, we did observe 20 crossover sequence types from both samplings, suggesting that there are STs well adapted to colonising the Australian silver gull. Multiple sub-lineages within these sequence types had low SNV counts among isolates recovered more than seven years apart (e.g. ST372 O21:H14 at 81–114 SNVs and ST624 O1:H1 at 91 SNVs). In addition, we identified ST624 from both 2012 and 2019 that encode the *intI1*_{Δ682}

truncation and carrying F18:A5:B1 ColV plasmids. This same deletion signature was also observed in recently emerged pandemic *E. coli* ST1193 (Wyrsh et al., 2022b). Various IS26-mediated *intI1* truncation signatures including *intI1*_{Δ682}, *intI1*_{Δ1006} and *intI1*_{Δ828} that were prevalent in the 2012 dataset, were also identified in the 2019 study reported here. These may be useful targets for the development of diagnostic assays to monitor AMR in wildlife populations that are impacted by human activity.

A high degree of ExPEC virulence gene carriage was observed in the 2019 collection, including the identification of several F plasmids that carry unusual virulence gene cargo. Adhesins, toxins, and iron capture systems underpin virulence in ExPEC (Poolman and Wacker, 2016) and it remains a challenge to identify emerging ExPEC lineages before they evolve to become pandemic lineages. ExPEC are colonising

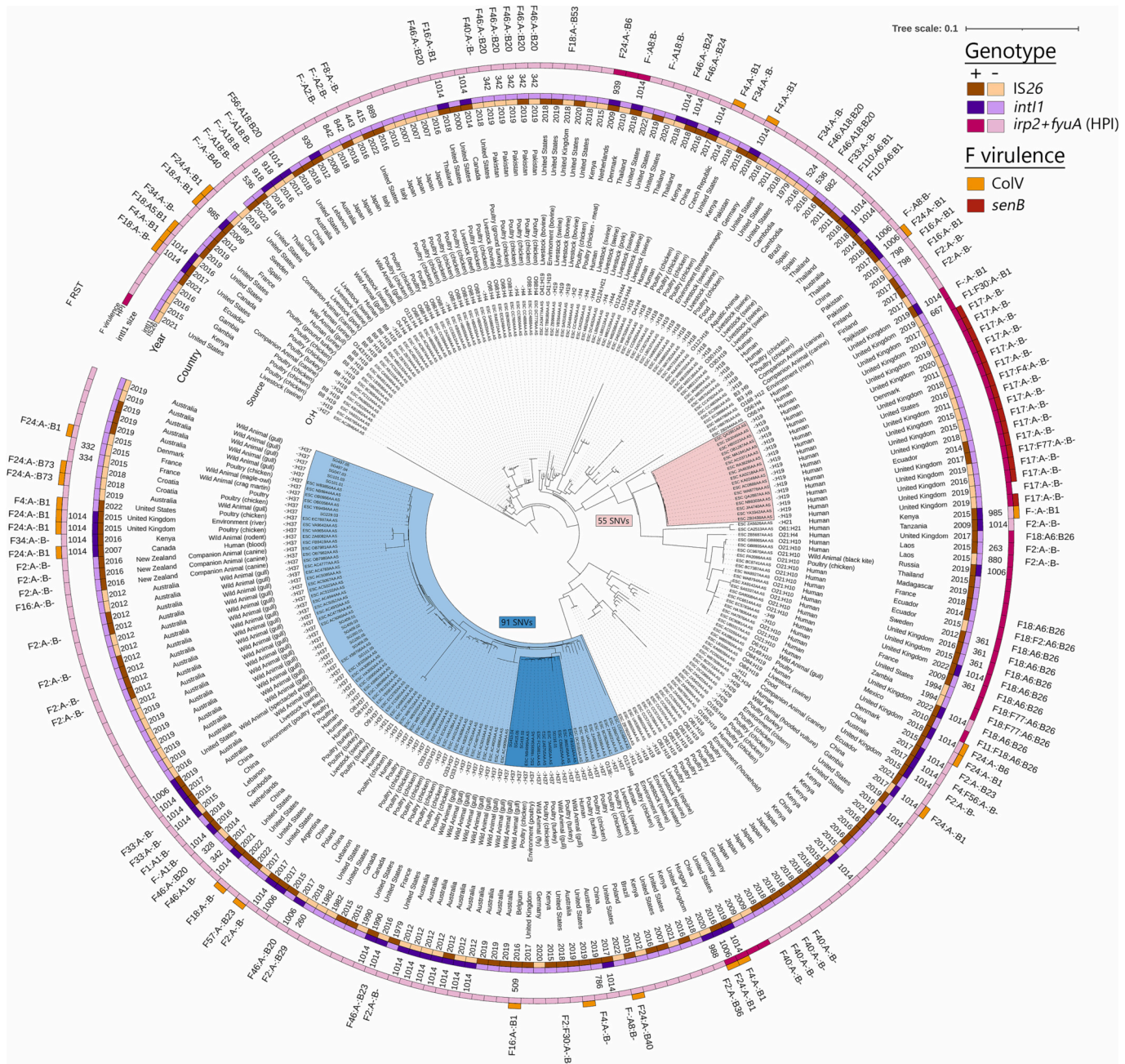


Fig. 8. A mid-point rooted maximum likelihood phylogenetic tree of *E. coli* 236 ST746 isolates from this study and reference isolates, generated using Parsnp based on 67,976 variant sites. Reference sequences and metadata were sourced from Enterobase. Data includes isolate source and year, detected serotype (O:H), *int1* hit (BLASTn match size to *int1* reference) and squares indicating gene presence/absence, where darker colours indicate positive detection for labelled genes and virulence markers. Colour-coded maximum SNV counts of selected subclades are included.

opportunistic pathogens and as such there can be a considerable time period between a colonisation event and the precipitation of a disease event or outbreak (Price et al., 2017). MGEs play a critical role in ExPEC virulence through the acquisition of F virulence plasmids, genomic islands and phages, often in combination (Cummins et al., 2022; Reid et al., 2022; Diard et al., 2010). However the acquisition and stable inheritance of these MGEs is typically lineage-specific and poorly understood (Cummins et al., 2022; Royer et al., 2023; Reid et al., 2022). The *Yersinia* High Pathogenicity Island is a chromosomally hosted virulence region, identified genotypically by the presence of siderophore genes *irp2* and *fyuA* (Tu et al., 2016) and is significant in this regard. The presence of HPI is ranked highly in lineages that cause ExPEC disease in mouse models of sepsis and blood stream infections (Galardini et al.,

2020; Royer et al., 2023; J.R. Johnson et al., 2006; G. Li et al., 2023) and is found in a diverse range of ExPEC lineages and other *Enterobacteriaceae* (Wyrsh et al., 2022a; Fonseca et al., 2022; Mokracka et al., 2004; Dos Santos et al., 2021). Yersiniabactin is an important siderophore and in innate immune cells has been shown to reduce the respiratory oxidative stress response (Paauw et al., 2009). It has also been linked with trace metal acquisition including iron, copper, and nickel (Robinson et al., 2018; Katumba et al., 2022), and influences strain motility (Magistro et al., 2017), suggesting it plays a critical role in microbial host fitness during extraintestinal infections. In our current study, HPI was identified in over one third of the collection (169 isolates; 39%). Apart from phylogroup B2, key lineages in the 2019 collection that hosted the island included ST457 (phylogroup F), ST68 and ST1143

from phylogroup D, ST58 from phylogroup B1, and ST88 (O9:H4 but not O8:H9) and ST1671 from phylogroup C. Many of these sequence types, including ST457, ST58, ST68, ST88, have been associated with ExPEC disease in humans (Nesporova et al., 2020; Reid et al., 2022; Chen et al., 2014; Amulele et al., 2023). Other sporadic sequence types carrying HPI were also noted. Despite the high levels of lineage diversity in both of our gull studies, both comprised of 30–40 % isolates encoding the HPI. In addition, F virulence plasmids were prominent in our collection with 52 isolates (15 STs; 58 % carrying HPI) carrying a bona fide ColV plasmid, 62 isolates carrying a ColV-like plasmid with a SPATE (16 STs; 90 % carry HPI) and 9 isolates, all with HPI, with *cjrABC-senB* plasmid F29:A-B10. In total, 123 isolates (28.5 %) in the 2019 collection harbour an F virulence plasmid with ExPEC virulence gene cargo, the vast majority of which also harbour HPI. Collectively, these findings implicate the silver gull as a prominent host of potential ExPEC pathogens.

Of the 62 isolates carrying a ColV-like SPATE plasmid, 49 reside in phylogroup B2 and most displayed an FII-64 replicon type. These plasmids were identified in ST978 (11 isolates; O4:H27), ST8611 (8 isolates; O113:H5), ST538 (6 isolates, O129-O13:H4), ST6530 (6 isolates; O17:H5), ST1868 (4 isolates), ST681 (4 isolates; mixed serotypes), ST1860, (3 isolates), ST8464 (3 isolates), ST131 O62:H4 (1 isolate), ST1597 (1 isolate), ST1857 (1 isolate) and ST1858 (1 isolate). The remaining 13 isolates carrying a ColV-like plasmid with Sha were spread among phylogroup A including ST14125 (2 isolates), phylogroup B1 ST1611 (5 isolates) and ST155 (1 isolate) and phylogroup F ST457 (5 isolates). Of these, ST131, ST155, ST457, ST538, ST978, ST681, ST1597, ST1868 have previously been linked to human carriage and often in association with ExPEC infection (UTI or BSI) (Hertz et al., 2016; Piazza et al., 2021; Maluta et al., 2014). In one epidemiological study, ColV-like SPATE plasmids that carry the autotransporter Sha were identified in 1 % of UPEC and 20 % of avian pathogenic *E. coli* (Habouria et al., 2019). Nonetheless, ExPEC lineages that carry HPI and ColV and related F plasmids including F64 F virulence plasmids pose an emerging threat to human and animal health. We recommend that these lineages be monitored closely in One Health surveillance programs.

The most striking difference between ExPEC virulence carriage in the 2012 and 2019 sampling data stems from the plethora of previously unobserved B2 lineages (and some isolates from other phylogroups) that were host to an F virulence plasmid very rarely observed in our 2012 study. Indeed there were only 9 entries in GenBank describing similar plasmids, including from a blood stream infection (Amadesi et al., 2023). Although ColV-like SPATE plasmids carrying Sha and other autotransporter proteins have been identified and isolated from poultry in France (Habouria et al., 2019), our data suggests that the Australian silver gull may represent an important, yet underappreciated, wildlife host of this unusual F virulence plasmid. Generally denoted by an FII-64 RST subtype, this plasmid family encodes a range of genes usually associated with ColV virulence plasmids (*iro*, *ets*, *hlyF*, *ompT*), plus an additional SPATE (*sha*) virulence operon (Pokharel et al., 2020) as well as carriage of *pap* operons. Detailed analysis and comparison to reference plasmids of similar genotype and F RST indicates that this series of plasmids are an off-shoot of a distinct ColV plasmid, with the noted variability in the *hlyF* allele a potentially useful marker for identifying this plasmid lineage. Further investigation to observe if different *hlyF* alleles are found predominantly in avian versus human ExPEC pathogens is warranted. Whether this plasmid's absence in the 2012 collection is a result of antibiotic selection bias, or whether it is a plasmid that has more recently begun to dominate the silver gull population nesting on Big Island requires further investigation. Nonetheless, isolation of *E. coli* carrying these unusual ColV-like SPATE plasmids suggests they are present in waste streams, including municipal waste sites and sewage outflows (and hence the local human population), that are frequented by silver gulls nesting on Big Island.

Previous studies have demonstrated a strong association between carriage of the HPI in *E. coli* phylogroups B2 and D, and sporadic,

lineage-specific carriage among the other major phylogroups (Clermont et al., 2001). In our prior analysis of critically drug resistant *E. coli* from the Australian silver gull (2012), we saw a similar distribution of HPI across the phylogroups, although sampling for that study did not result in the recovery of many group B2 isolates. From the 2012 collection, ST457 (group F) was a major contributor to total HPI carriage, with ST23 and ST88 from group C being other notable carriers of the island. All these sequence types are notable in their ability to cause serious human disease. A subset of F plasmids that encode *cjrABC-senB* virulence gene cargo, historically typed as F29:A-B10 plasmids but now associated with multiple F RSTs, are dominant in many major ExPEC pandemic lineages including ST131 clades A, B and C1 (Li et al., 2021; Johnson et al., 2016), ST127 (Elankumaran et al., 2022b), ST95 (Cummins et al., 2022), and recently emerged ExPEC sequence types including ST1193 (Wyrsh et al., 2022b; J.R. Johnson et al., 2019; T.J. Johnson et al., 2019), and ST963 which is a dominant *bla*_{CMY-2} carrying lineage in Australian gulls (Medvecky et al., 2022). Only 9 isolates spanning three sequence types carry *cjrABC-senB* in our 2019 collection: ST58 (5 isolates from same sample), ST10 (3 isolates from same sample) and ST162 (1 isolate). This is in stark contrast to the 2012 collection where 45 (10.6 %) isolates carried *cjrABC-senB* plasmids that showed sequence identity with pUTI89. It is noteworthy however that this discrepancy between the two collections was predominantly due to the frequent appearance of cefotaxime-resistant ST963 in the 2012 sampling encoding a chromosomal copy of *bla*_{CMY-2} (Medvecky et al., 2022).

To demonstrate the relevance of these ExPEC and AMR markers, we provide phylogenetic analyses and genotyping of three ExPEC sequence types noted for their emerging virulence: ST58 (Reid et al., 2022; McKinnon et al., 2018; Jamborova et al., 2015), ST457 (Nesporova et al., 2020; Nesporova et al., 2021), and ST746 (Yang et al., 2022) that are well represented in our collections. Through these analyses, we highlight numerous *E. coli* lineages hosting ExPEC virulence factors and AMR and identified instances where isolates from different sources (frequently wild birds, humans, and companion animals) were closely related, defined here as SNV differences <100 (Table 2). These sequence types have been linked with extraintestinal disease in humans and are known to circulate in wild or domesticated birds (Yang et al., 2022; Wyrsh et al., 2020; Han et al., 2021).

To explore any relevant relationships between gull isolates and those available in public databases, we performed comparative phylogenomic analyses against publicly available ST58 (Australian data only), ST457 and ST746 isolates. The distribution of ST58 isolates was indicative of multiple lineages circulating within Australia, with a broad presence of AMR-associated factors and significant ExPEC potential, particularly within a subset of phylogenetically related lineages. This analysis also demonstrated some One Health linkages, between canine, wild bird (gull and ibis) and human isolates. Expanding this type of analysis to the international ST457 data, we were able to demonstrate the existence of multiple globally disseminated ExPEC lineages and many subclades linked by F plasmid and class 1 integron carriage (Fig. 7). We observed some clear distinctions between HPI-encoding and non-encoding subclades within the sequence type, with all gull isolates from this study included within the HPI-encoding clades. ST457 was also a dominant phylogroup F lineage in our 2012 study. Taken together, with links to global poultry production (Nesporova et al., 2020; Han et al., 2021), the data served to indicate that ST457 is an avian-adapted lineage with substantial virulence potential. In addition, ST457 is capable of carrying genes encoding resistance to clinically important antibiotics. While the genotypes appeared less consistent within the ST746 analysis (an indication of higher levels of diversity within the sequence type), various clades were still demonstrated to be potential ExPEC and examples of One Health-type epidemiological links were found. ST372 was identified in both the 2012 and 2019 sampling and is a frequently identified *E. coli* sequence type in dogs (Elankumaran et al., 2023), an interspecies linkage this study has helped provide some evidence for.

Detection of multiple variants of the tLST among diverse *E. coli*

lineages belonging to phylogroups A and B1 aligns with previous reports of tLST distribution (Zhang and Yang, 2022; Mercer et al., 2015) but detection of tLST in the Australian silver gull is novel, and points to urban birds being an important, yet underappreciated source of *E. coli* that carry this sanitation resistance locus. While co-carriage of HPI was limited in isolates carrying tLST it highlights the diversity of *E. coli* that carry important virulence gene cargo. Further studies are needed to determine if isolates that carry tLST represent enteric *E. coli* lineages that are adapting to survive wastewater sanitation methods as described elsewhere in other parts of the world or are they naturalised lineages of *E. coli* that have evolved in wastewater streams (Wang et al., 2020). Birds have a significantly higher body temperature than most vertebrates and may represent a natural host for *E. coli* that carry tLST. It is also feasible that *E. coli* have acquired tLST to survive urban heat islands (Zhao et al., 2014; Zhou et al., 2014). Faecal excrement from urban birds, companion animals and rodents contaminates urban pavements and urban runoff may represent a substantial source of *E. coli* carrying tLST (Müller et al., 2020). Almost all the *E. coli* isolates from 2012 carrying tLST, isolated based on phenotypic resistance to one of three clinically important antibiotics, also carried a class 1 integron and were genotypically multiple drug resistant (Table 1) while those from the 2019 collection did not.

In conclusion, the Australian Silver Gull has been shown to host an extremely diverse variety of *E. coli* lineages with a high presence of both potential ExPEC and critical drug resistances, depending on isolation method. This study highlights how studies that focus on antimicrobial resistance may generate bias and obfuscates deeper understanding of virulence carriage and thereby pathogen evolution more generally (Djordjevic, 2023). To monitor and prevent the continuing expansion of ExPEC-mediated disease and antimicrobial resistance, urban-adapted wild birds must be considered an important host of potential pathogens and a highly mobile source of *E. coli* with the capacity to carry resistance to clinically important antibiotics (Wyrsh et al., 2022a).

Supplementary data to this article can be found online at <https://doi.org/10.1016/j.scitotenv.2024.170815>.

Funding

This project was funded by the Australian Centre for Genomic Epidemiological Microbiology (AusGEM), a collaborative partnership between the NSW Department of Primary Industries and the University of Technology Sydney (S.P.D.), a target grant from the University of Wollongong Faculty of Science, Medicine and Health (B.J.H.), and a Nisbet research grant from the Waterbird Society (K.M.).

CRediT authorship contribution statement

Ethan R. Wyrsh: Writing – review & editing, Writing – original draft, Visualization, Methodology, Investigation, Formal analysis, Data curation. **Bethany J. Hoye:** Writing – review & editing, Writing – original draft, Supervision, Funding acquisition, Data curation, Conceptualization. **Martina Sanderson-Smith:** Writing – review & editing, Investigation. **Jody Gorman:** Investigation. **Kimberly Maute:** Investigation. **Max L. Cummins:** Methodology, Data curation. **Veronica M. Jarocki:** Writing – review & editing, Validation, Methodology. **Marc S. Marenda:** Writing – review & editing, Methodology, Investigation. **Monika Dolejska:** Writing – review & editing, Supervision, Data curation, Conceptualization. **Steven P. Djordjevic:** Writing – review & editing, Writing – original draft, Supervision, Project administration, Funding acquisition, Conceptualization.

Declaration of competing interest

The authors declare that they have no known competing financial interests or personal relationships that could have appeared to influence the work reported in this paper.

Data availability

All whole genome sequences generated for this study are available under GenBank BioProject PRJNA1037278.

References

- Ahlstrom, C.A., et al., 2019. Satellite tracking of gulls and genomic characterization of faecal bacteria reveals environmentally mediated acquisition and dispersal of antimicrobial-resistant *Escherichia coli* on the Kenai Peninsula, Alaska. *Molecular Ecology* 28, 2531–2545.
- Ahlstrom, C.A., et al., 2021. Evidence for continental-scale dispersal of antimicrobial resistant bacteria by landfill-foraging gulls. *Sci. Total Environ.* 764, 144551.
- Albery, G.F., et al., 2022. Urban-adapted mammal species have more known pathogens. *Nature Ecology & Evolution* 6, 794–801.
- Alikhan, N.F., Petty, N.K., Ben Zakour, N.L., Beatson, S.A., 2011. BLAST Ring Image Generator (BRIG): simple prokaryote genome comparisons. *BMC Genomics* 12, 402.
- Amadesi, S., et al., 2023. Severe *Escherichia coli* infections in critical adult patients: two case reports and genomic analysis. *New Microbiol.* 46, 24–28.
- Amulele, A.V., et al., 2023. Recurrent spontaneous *Escherichia coli* meningitis in an adult: a case report. *JAC-Antimicrobial Resistance* 5.
- Banerjee, R., et al., 2013. The clonal distribution and diversity of extraintestinal *Escherichia coli* isolates vary according to patient characteristics. *Antimicrob. Agents Chemother.* 57, 5912–5917.
- Becker, D.J., Hall, R.J., 2014. Too much of a good thing: resource provisioning alters infectious disease dynamics in wildlife. *Biol. Lett.* 10.
- Bolzoni, L., De Leo, G.A., 2013. Unexpected consequences of culling on the eradication of wildlife diseases: the role of virulence evolution. *Am. Nat.* 181, 301–313.
- Camacho, C., et al., 2009. BLAST+: architecture and applications. *BMC Bioinformatics* 10, 421.
- Carattoli, A., et al., 2014. *In silico* detection and typing of plasmids using PlasmidFinder and plasmid multilocus sequence typing. *Antimicrob. Agents Chemother.* 58, 3895–3903.
- Chen, L., et al., 2005. VFDB: a reference database for bacterial virulence factors. *Nucleic Acids Res.* 33, D325–D328.
- Chen, C.M., Ke, S.C., Li, C.R., Chiou, C.S., Chang, C.C., 2014. Prolonged clonal spreading and dynamic changes in antimicrobial resistance of *Escherichia coli* ST68 among patients who stayed in a respiratory care ward. *J. Med. Microbiol.* 63, 1531–1541.
- Clermont, O., Bonacorsi, S., Bingen, E., 2001. The *Yersinia* high-pathogenicity island is highly predominant in virulence-associated phylogenetic groups of *Escherichia coli*. *FEMS Microbiol. Lett.* 196, 153–157.
- Cummins, M.L., et al., 2020. Whole-genome sequence analysis of an extensively drug-resistant *Salmonella enterica* serovar Agona isolate from an Australian silver gull (*Chroicocephalus novaehollandiae*) reveals the acquisition of multidrug resistance plasmids. *mSphere* 5.
- Cummins, M.L., Reid, C.J., Djordjevic, S.P., 2022. F plasmid lineages in *Escherichia coli* ST95: implications for host range, antibiotic resistance, and zoonoses. *mSystems* 7, e0121221.
- Cusumano, C.K., Hung, C.S., Chen, S.L., Hultgren, S.J., 2010. Virulence plasmid harbored by uropathogenic *Escherichia coli* functions in acute stages of pathogenesis. *Infect. Immun.* 78, 1457–1467.
- Darling, A.E., Mau, B., Perna, N.T., 2010. progressiveMauve: multiple genome alignment with gene gain, loss and rearrangement. *PLoS One* 5, e11147.
- Darling, A.E., et al., 2014. PhyloSift: phylogenetic analysis of genomes and metagenomes. *PeerJ* 2, e243.
- Diard, M., et al., 2010. Pathogenicity-associated islands in extraintestinal pathogenic *Escherichia coli* are fitness elements involved in intestinal colonization. *J. Bacteriol.* 192, 4885–4893.
- Dias, D., Fonseca, C., Caetano, T., Mendo, S., 2022. Oh, deer! How worried should we be about the diversity and abundance of the faecal resistome of red deer? *Sci. Total Environ.* 825, 153831.
- Dolejska, M., Literak, I., 2019. Wildlife is overlooked in the epidemiology of medically important antibiotic-resistant bacteria. *Antimicrob. Agents Chemother.* 63.
- Djordjevic, S.P., 2023. Genomic surveillance for antimicrobial resistance — a One Health perspective. *Nat. Rev. Genet.* 25, 142–157.
- Dolejska, M., et al., 2016. High prevalence of *Salmonella* and IMP-4-producing Enterobacteriaceae in the silver gull on Five Islands, Australia. *J. Antimicrob. Chemother.* 71, 63–70.
- Dos Santos, A.M.P., Ferrari, R.G., Panzenhagen, P., Rodrigues, G.L., Conte-Junior, C.A., 2021. Virulence genes identification and characterization revealed the presence of the *Yersinia* High Pathogenicity Island (HPI) in *Salmonella* from Brazil. *Gene* 787, 145646.
- Elankumaran, P., et al., 2022a. Genomic and temporal trends in canine ExPEC reflect those of human ExPEC. *Microbiol Spectr* 10, e0129122.
- Elankumaran, P., Browning, G.F., Marenda, M.S., Reid, C.J., Djordjevic, S.P., 2022b. Close genetic linkage between human and companion animal extraintestinal pathogenic *Escherichia coli* ST127. *Current Research in Microbial Sciences* 3, 100106.
- Elankumaran, P., et al., 2023. Identification of genes influencing the evolution of *Escherichia coli* ST372 in dogs and humans. *Microb Genom* 9.
- Fonseca, E.L., Morgado, S.M., Caldart, R.V., Vicente, A.C., 2022. Global genomic epidemiology of *Escherichia coli* (ExPEC) ST38 lineage revealed a Virulome associated with human infections. *Microorganisms* 10, 2482.

- Furness, L.E., Campbell, A., Zhang, L., Gaze, W.H., McDonald, R.A., 2017. Wild small mammals as sentinels for the environmental transmission of antimicrobial resistance. *Environ. Res.* 154, 28–34.
- Gaio, D., et al., 2022. Hackflex: low-cost, high-throughput, Illumina Nextera Flex library construction. *Microb. Genom.* 8.
- Gajdosova, J., et al., 2011. Analysis of the DNA region mediating increased thermotolerance at 58°C in *Cronobacter* sp. and other enterobacterial strains. *Antonie Van Leeuwenhoek* 100, 279–289.
- Galardini, M., et al., 2020. Major role of iron uptake systems in the intrinsic extra-intestinal virulence of the genus *Escherichia* revealed by a genome-wide association study. *PLoS Genet.* 16, e1009065.
- Guragain, M., Brichta-Harhay, D.M., Bono, J.L., Bosilevac, J.M., 2021. Locus of heat resistance (LHR) in meat-borne *Escherichia coli*: screening and genetic characterization. *Appl. Environ. Microbiol.* 87.
- Habouria, H., et al., 2019. Three new serine-protease autotransporters of Enterobacteriaceae (SPATEs) from extra-intestinal pathogenic *Escherichia coli* and combined role of SPATEs for cytotoxicity and colonization of the mouse kidney. *Virulence* 10, 568–587.
- Han, L., et al., 2021. Molecular epidemiology of fosfomycin resistant *E. coli* from a pigeon farm in China. *Antibiotics* 10, 777.
- Harmer, C.J., Moran, R.A., Hall, R.M., 2014. Movement of IS26-associated antibiotic resistance genes occurs via a translocatable unit that includes a single IS26 and preferentially inserts adjacent to another IS26. *mBio* 5, e01801-14.
- Hassell, J.M., Begon, M., Ward, M.J., Fèvre, E.M., 2017. Urbanization and disease emergence: dynamics at the wildlife-livestock-human interface. *Trends Ecol. Evol.* 32, 55–67.
- Hassell, J.M., et al., 2019. Deterministic processes structure bacterial genetic communities across an urban landscape. *Nat. Commun.* 10, 2643.
- Hertz, F.B., et al., 2016. Population structure of drug-susceptible, -resistant and ESBL-producing *Escherichia coli* from community-acquired urinary tract infections. *BMC Microbiol.* 16, 63.
- Jamborova, I., et al., 2015. Plasmid-mediated resistance to cephalosporins and fluoroquinolones in various *Escherichia coli* sequence types isolated from rooks wintering in Europe. *Appl. Environ. Microbiol.* 81, 648–657.
- Joensen, K., Tetzschner, A., Iguchi, A., Aarestrup, F., Scheut, F., 2015. Rapid and easy in silico serotyping of *Escherichia coli* isolates by use of whole-genome sequencing data. *J. Clin. Microbiol.* 53, 2410–2426.
- Johnson, T.J., Nolan, L.K., 2009. Pathogenomics of the virulence plasmids of *Escherichia coli*. *Mol. Biol. Rev.* 73, 750–774.
- Johnson, T.J., Siek, K.E., Johnson, S.J., Nolan, L.K., 2006a. DNA sequence of a ColV plasmid and prevalence of selected plasmid-encoded virulence genes among avian *Escherichia coli* strains. *J. Bacteriol.* 188, 745–758.
- Johnson, J.R., et al., 2006b. Experimental mouse lethality of *Escherichia coli* isolates, in relation to accessory traits, phylogenetic group, and ecological source. *J. Infect. Dis.* 194, 1141–1150.
- Johnson, T.J., et al., 2016. Separate F-type plasmids have shaped the evolution of the H30 subclone of *Escherichia coli* sequence type 131. *mSphere* 1, e00121-16.
- Johnson, J.R., et al., 2018. Contribution of yersiniabactin to the virulence of an *Escherichia coli* sequence type 69 (“clonal group A”) cystitis isolate in murine models of urinary tract infection and sepsis. *Microb. Pathog.* 120, 128–131.
- Johnson, J.R., et al., 2019a. Rapid emergence, subsidence, and molecular detection of *Escherichia coli* sequence type 1193-fimH64, a new disseminated multidrug-resistant commensal and extraintestinal pathogen. *J. Clin. Microbiol.* 57, e01664-18.
- Johnson, T.J., et al., 2019b. Phylogenomic analysis of extraintestinal pathogenic *Escherichia coli* sequence type 1193, an emerging multidrug-resistant clonal group. *Antimicrob. Agents Chemother.* 63.
- Jolley, K.A., Bray, J.E., Maiden, M.C.J., 2018. Open-access bacterial population genomics: BIGSdb software, the PubMLST.org website and their applications. *Wellcome Open Res* 3, 124.
- Katumba, G.L., Tran, H., Henderson, J.P., 2022. The Yersinia high-pathogenicity island encodes a siderophore-dependent copper response system in uropathogenic *Escherichia coli*. *mBio* 13, e0239121.
- Lagerstrom, K.M., Hadly, E.A., 2021. The under-investigated wild side of *Escherichia coli*: genetic diversity, pathogenicity and antimicrobial resistance in wild animals. *Proc. R. Soc. B Biol. Sci.* 288, 20210399.
- Letunic, I., Bork, P., 2019. Interactive Tree Of Life (iTOL) v4: recent updates and new developments. *Nucleic Acids Res.* 47, W256–w259.
- Li, D., et al., 2021. Genomic comparisons of *Escherichia coli* ST131 from Australia. *Microb. Genom.* 7.
- Li, D., et al., 2023a. Dominance of *Escherichia coli* sequence types ST73, ST95, ST127 and ST131 in Australian urine isolates: a genomic analysis of antimicrobial resistance and virulence linked to F plasmids. *Microb. Genom.* 9.
- Li, G., Li, M., Yu, D., Sun, W., 2023b. Effect of high-pathogenicity island (HPI) on TGF- β 1/Smad3 pathway in mouse model of *E. coli* strains causing diarrhea in calf. *Res. Vet. Sci.* 156, 1–6.
- Liu, C.M., et al., 2018. *Escherichia coli* ST131-H22 as a foodborne uropathogen. *mBio* 9.
- Ma, A., Glassman, H., Chui, L., 2020. Characterization of *Escherichia coli* possessing the locus of heat resistance isolated from human cases of acute gastroenteritis. *Food Microbiol.* 88, 103400.
- Magistro, G., Magistro, C., Stief, C.G., Schubert, S., 2017. The high-pathogenicity island (HPI) promotes flagellum-mediated motility in extraintestinal pathogenic *Escherichia coli*. *PLoS One* 12, e0183950.
- Maluta, R.P., et al., 2014. Overlapped sequence types (STs) and serogroups of avian pathogenic (APEC) and human extra-intestinal pathogenic (ExPEC) *Escherichia coli* isolated in Brazil. *PLoS One* 9, e105016.
- Manges, A.R., et al., 2019. Global extraintestinal pathogenic *Escherichia coli* (ExPEC) lineages. *Clin. Microbiol. Rev.* 32.
- McKinnon, J., Roy Chowdhury, P., Djordjevic, S.P., 2018. Genomic analysis of multidrug-resistant *Escherichia coli* ST58 causing urosepsis. *Int. J. Antimicrob. Agents* 52, 430–435.
- Medvecky, M., et al., 2022. Interspecies transmission of CMY-2-producing *Escherichia coli* sequence type 963 isolates between humans and gulls in Australia. *mSphere* 7, e0023822.
- Mercer, R.G., et al., 2015. Genetic determinants of heat resistance in *Escherichia coli*. *Front. Microbiol.* 6, 932.
- Mercer, R., Nguyen, O., Ou, Q., McMullen, L., Gänze, M.G., 2017. Functional analysis of genes comprising the locus of heat resistance in *Escherichia coli*. *Appl. Environ. Microbiol.* 83.
- Mokracka, J., Koczura, R., Kaznowski, A., 2004. Yersiniabactin and other siderophores produced by clinical isolates of *Enterobacter* spp. and *Citrobacter* spp. *FEMS Immunology & Medical Microbiology* 40, 51–55.
- Morales, C., Lee, M.D., Hofacre, C., Maurer, J.J., 2004. Detection of a novel virulence gene and a *Salmonella* virulence homologue among *Escherichia coli* isolated from broiler chickens. *Foodborne Pathog. Dis.* 1, 160–165.
- Mukerji, S., et al., 2019. Resistance to critically important antimicrobials in Australian silver gulls (*Chroicocephalus novaehollandiae*) and evidence of anthropogenic origins. *J. Antimicrob. Chemother.* 74, 2566–2574.
- Mukerji, S., et al., 2020. Implications of foraging and interspecies interactions of birds for carriage of *Escherichia coli* strains resistant to critically important antimicrobials. *Appl. Environ. Microbiol.* 86.
- Mukerji, S., et al., 2023. Proximity to human settlement is directly related to carriage of critically important antimicrobial-resistant *Escherichia coli* and *Klebsiella pneumoniae* in Silver Gulls. *Vet. Microbiol.* 280, 109702.
- Müller, A., Österlund, H., Marsalek, J., Viklander, M., 2020. The pollution conveyed by urban runoff: a review of sources. *Sci. Total Environ.* 709, 136125.
- Murase, K., et al., 2016. HlyF produced by extraintestinal pathogenic *Escherichia coli* is a virulence factor that regulates outer membrane vesicle biogenesis. *J. Infect. Dis.* 213, 856–865.
- Nesporova, K., et al., 2020. *Escherichia coli* sequence type 457 is an emerging extended-spectrum- β -lactam-resistant lineage with reservoirs in wildlife and food-producing animals. *Antimicrob. Agents Chemother.* 65.
- Nesporova, K., et al., 2021. Multi-drug resistant plasmids with ESBL/AmpC and mcr-5.1 in Paraguayan poultry farms: the linkage of antibiotic resistance and hatcheries. *Microorganisms* 9.
- Paauw, A., Leverstein-van Hall, M.A., van Kessel, K.P., Verhoef, J., Fluit, A.C., 2009. Yersiniabactin reduces the respiratory oxidative stress response of innate immune cells. *PLoS One* 4, e8240.
- Partridge, S.R., Ginn, A.N., Paulsen, I.T., Iredell, J.R., 2012. pEI1573 carrying bla_{IMP-4}, from Sydney, Australia, is closely related to other IncL/M plasmids. *Antimicrob. Agents Chemother.* 56, 6029–6032.
- Piazza, A., et al., 2021. Whole-genome sequencing investigation of a large nosocomial outbreak caused by ST131 H30Rx KPC-producing *Escherichia coli* in Italy. *Antibiotics* 10, 718.
- Pokharel, P., et al., 2020. The serine protease autotransporters TagB, TagC, and Sha from extraintestinal pathogenic *Escherichia coli* are internalized by human bladder epithelial cells and cause actin cytoskeletal disruption. *Int. J. Mol. Sci.* 21.
- Poolman, J.T., Wacker, M., 2016. Extraintestinal pathogenic *Escherichia coli*, a common human pathogen: challenges for vaccine development and progress in the field. *J. Infect. Dis.* 213, 6–13.
- Price, M.N., Dehal, P.S., Arkin, A.P., 2010. FastTree 2—approximately maximum-likelihood trees for large alignments. *PLoS One* 5, e9490.
- Price, L.B., Hungate, B.A., Koch, B.J., Davis, G.S., Liu, C.M., 2017. Colonizing opportunistic pathogens (COPs): the beasts in all of us. *PLoS Pathog.* 13, e1006369.
- Ramey, A.M., Ahlstrom, C.A., 2020. Antibiotic resistant bacteria in wildlife: perspectives on trends, acquisition and dissemination, data gaps, and future directions. *J. Wildl. Dis.* 56, 1–15.
- Reid, C.J., et al., 2022. A role for ColV plasmids in the evolution of pathogenic *Escherichia coli* ST58. *Nat. Commun.* 13, 683.
- Robinson, A.E., Lowe, J.E., Koh, E.I., Henderson, J.P., 2018. Uropathogenic enterobacteria use the yersiniabactin metallophore system to acquire nickel. *J. Biol. Chem.* 293, 14953–14961.
- Rodríguez, I., et al., 2021. A 21-year survey of *Escherichia coli* from bloodstream infections (BSI) in a tertiary hospital reveals how community-hospital dynamics of B2 phylogroup clones influence local BSI rates. *mSphere* 6, e0086821.
- Royer, G., et al., 2023. Epistatic interactions between the high pathogenicity island and other iron uptake systems shape *Escherichia coli* extra-intestinal virulence. *Nat. Commun.* 14, 3667.
- Sabaté, M., Moreno, E., Pérez, T., Andreu, A., Prats, G., 2006. Pathogenicity island markers in commensal and uropathogenic *Escherichia coli* isolates. *Clin. Microbiol. Infect.* 12, 880–886.
- Schubert, S., Picard, B., Gouriou, S., Heesemann, J., Denamur, E., 2002. Yersinia high-pathogenicity island contributes to virulence in *Escherichia coli* causing extraintestinal infections. *Infect. Immun.* 70, 5335–5337.
- Seemann, T., 2014. Prokka: rapid prokaryotic genome annotation. *Bioinformatics* 30, 2068–2069.
- Skyberg, J.A., et al., 2006. Acquisition of avian pathogenic *Escherichia coli* plasmids by a commensal *E. coli* isolate enhances its abilities to kill chicken embryos, grow in human urine, and colonize the murine kidney. *Infect. Immun.* 74, 6287–6292.
- Stephens, C.M., Adams-Sapper, S., Sekhon, M., Johnson, J.R., Riley, L.W., 2017. Genomic analysis of factors associated with low prevalence of antibiotic resistance in extraintestinal pathogenic *Escherichia coli* sequence type 95 strains. *mSphere* 2.

- Stoppe, N.C., et al., 2017. Worldwide phylogenetic group patterns of *Escherichia coli* from commensal human and wastewater treatment plant isolates. *Front. Microbiol.* 8, 2512.
- Svanborg, C., Godaly, G., 1997. Bacterial virulence in urinary tract infection. *Infect. Dis. Clin. N. Am.* 11, 513–529.
- Tarabai, H., Wyrsh, E.R., Bitar, I., Dolejska, M., Djordjevic, S.P., 2021. Epidemic HI2 plasmids mobilising the carbapenemase gene bla(IMP-4) in Australian clinical samples identified in multiple sublineages of *Escherichia coli* ST216 colonising silver gulls. *Microorganisms* 9.
- Tarabai, H., 2023. Clinically relevant antibiotic resistance in *Escherichia coli* from black kites in southwestern Siberia: a genetic and phenotypic investigation. *mSphere* 8, e0009923.
- Torres, R.T., et al., 2021. Temporal and geographical research trends of antimicrobial resistance in wildlife - a bibliometric analysis. *One Health* 11, 100198.
- Treangen, T.J., Ondov, B.D., Koren, S., Phillippy, A.M., 2014. The Harvest suite for rapid core-genome alignment and visualization of thousands of intraspecific microbial genomes. *Genome Biol.* 15, 524.
- Tu, J., et al., 2016. The *irp2* and *fyuA* genes in High Pathogenicity Islands are involved in the pathogenesis of infections caused by avian pathogenic *Escherichia coli* (APEC). *Pol. J. Vet. Sci.* 19, 21–29.
- Uea-Anuwong, T., et al., 2023. Antimicrobial resistance in bacteria isolated from peridomestic *Rattus* species: a scoping literature review. *One Health* 16, 100522.
- Venturini, C., et al., 2019. Diversity of P1 phage-like elements in multidrug resistant *Escherichia coli*. *Sci. Rep.* 9, 18861.
- Wang, Z., et al., 2020. The locus of heat resistance confers resistance to chlorine and other oxidizing chemicals in *Escherichia coli*. *Appl. Environ. Microbiol.* 86, e02123-19.
- Wick, R.R., Judd, L.M., Gorrie, C.L., Holt, K.E., 2017. Unicycler: resolving bacterial genome assemblies from short and long sequencing reads. *PLoS Comput. Biol.* 13, e1005595.
- Wood, D.E., Lu, J., Langmead, B., 2019. Improved metagenomic analysis with Kraken 2. *Genome Biol.* 20, 257.
- Wyrsh, E.R., et al., 2020. Whole-genome sequence analysis of environmental *Escherichia coli* from the faeces of straw-necked ibis (*Threskiornis spinicollis*) nesting on inland wetlands. *Microb. Genom.* 6.
- Wyrsh, E.R., et al., 2022a. Urban wildlife crisis: Australian silver gull is a bystander host to widespread clinical antibiotic resistance. *mSystems* 7, e0015822.
- Wyrsh, E.R., Bushell, R.N., Marena, M.S., Browning, G.F., Djordjevic, S.P., 2022b. Global phylogeny and F virulence plasmid carriage in pandemic *Escherichia coli* ST1193. *Microbiol. Spectr.* 10, e0255422.
- Wyrsh, E.R., Dolejska, M., Djordjevic, S.P., 2022c. Genomic analysis of an II plasmid hosting a *sul3*-class I integron and blaSHV-12 within an unusual *Escherichia coli* ST297 from urban wildlife. *Microorganisms* 10, 1387.
- Yang, M., Xu, G., Ruan, Z., Wang, Y., 2022. Genomic characterization of a multidrug-resistant *Escherichia coli* isolate co-carrying bla (NDM-5) and bla (CTX-M-14) genes recovered from a pediatric patient in China. *Infect. Drug Resist.* 15, 6405–6412.
- Yu, D., Ryu, K., Zhi, S., Otto, S.J.G., Neumann, N.F., 2022. Naturalized *Escherichia coli* in wastewater and the co-evolution of bacterial resistance to water treatment and antibiotics. *Front. Microbiol.* 13, 810312.
- Zankari, E., et al., 2012. Identification of acquired antimicrobial resistance genes. *J. Antimicrob. Chemother.* 67, 2640–2644.
- Zhang, P., Yang, X., 2022. Genetic characteristics of the transmissible locus of stress tolerance (tLST) and tLST harboring *Escherichia coli* as revealed by large-scale genomic analysis. *Appl. Environ. Microbiol.* 88, e02185-21.
- Zhang, W.L., et al., 2002. Genetic diversity of intimin genes of attaching and effacing *Escherichia coli* strains. *J. Clin. Microbiol.* 40, 4486–4492.
- Zhao, L., Lee, X., Smith, R.B., Oleson, K., 2014. Strong contributions of local background climate to urban heat islands. *Nature* 511, 216–219.
- Zhou, D., Zhao, S., Liu, S., Zhang, L., Zhu, C., 2014. Surface urban heat island in China's 32 major cities: spatial patterns and drivers. *Remote Sens. Environ.* 152, 51–61.
- Zhou, Z., Alikhan, N.F., Mohamed, K., Fan, Y., Achtman, M., 2020. The Enterobase user's guide, with case studies on *Salmonella* transmissions, *Yersinia pestis* phylogeny, and *Escherichia coli* genomic diversity. *Genome Res.* 30, 138–152.